PLOS GENETICS

RESEARCH ARTICLE

An allelic series at the *EDNRB2* locus controls diverse piebalding patterns in the domestic pigeon

Emily T. Maclary, Ryan Wauer, Bridget Phillips, Audrey Brown, Elena F. Boer, Atoosa M. Samani, Michael D. Shapiro*

School of Biological Sciences, University of Utah, Salt Lake City, Utah, United States of America

* mike.shapiro@utah.edu

Citation: Maclary ET, Wauer R, Phillips B, Brown A, Boer EF, Samani AM, et al. (2023) An allelic series at the *EDNRB2* locus controls diverse piebalding patterns in the domestic pigeon. PLoS Genet 19(10): e1010880. https://doi.org/10.1371/journal.pgen.1010880

Editor: Gregory S. Barsh, HudsonAlpha Institute for Biotechnology, UNITED STATES

Received: July 25, 2023

Accepted: September 25, 2023

Published: October 20, 2023

Data Availability Statement: Whole genome sequencing and RNA-sequencing datasets generated for this study have been deposited to the NCBI SRA database under BioProject PRJNA986561 and are available at https://www.ncbi.nlm.nih.gov/bioproject/PRJNA986561. Previously generated whole genome sequencing data used in this study are available under BioProject accessions PRJNA680754, PRJNA513877, PRJNA428271, and PRJNA167554. Phenotyping data underlying the boxplots in Fig 1I and Fig 2, the PCA in S1 Fig, and

Abstract

Variation in pigment patterns within and among vertebrate species reflects underlying changes in cell migration and function that can impact health, reproductive success, and survival. The domestic pigeon (*Columba livia*) is an exceptional model for understanding the genetic changes that give rise to diverse pigment patterns, as selective breeding has given rise to hundreds of breeds with extensive variation in plumage color and pattern. Here, we map the genetic architecture of a suite of pigmentation phenotypes known as piebalding. Piebalding is characterized by patches of pigmented and non-pigmented feathers, and these plumage patterns are often breed-specific and stable across generations. Using a combination of quantitative trait locus mapping in F_2 laboratory crosses and genome-wide association analysis, we identify a locus associated with piebalding across many pigeon breeds. This shared locus harbors a candidate gene, *EDNRB2*, that is a known regulator of pigment cell migration, proliferation, and survival. We discover multiple distinct haplotypes at the *EDNRB2* locus in piebald pigeons, which include a mix of protein-coding, noncoding, and structural variants that are associated with depigmentation in specific plumage regions. These results identify a role for *EDNRB2* in pigment patterning in the domestic pigeon, and highlight how repeated selection at a single locus can generate a diverse array of stable and heritable pigment patterns.

Author summary

Both wild and domestic birds show striking variation in pigment patterning, and these pigment patterns can play critical roles in mate choice, communication, and camouflage. Despite the importance of pigment patterning for survival and reproductive success, the mechanisms that control pigment patterning remain incompletely understood. In domestic pigeons, artificial selection has given rise to a wide array of pigmentation patterns within a single species, including a suite of phenotypes called "piebalding" that is characterized by regional loss of feather pigment. Here, we took advantage of the wide array of distinct piebalding phenotypes in domestic pigeons to map the genetic basis of region-specific loss of plumage pigment. Rather than focusing on a single piebalding pattern, we

the PCAs and correlation heatmaps in S2 Fig are available in S1 Table.

Funding: This work was supported by the National Institutes of Health (R35GM131787 to M.D.S.; fellowship T32GM141848 to A.M.S.), a fellowship from the Jane Coffin Childs Memorial Fund for Medical Research (E.T.M.), and the University of Utah Undergraduate Research Opportunity Program (fellowship support to B.P. and R.W.). The funders had no role in study design, data collection and analysis, decision to publish, or preparation of the manuscript.

Competing interests: The authors have declared that no competing interests exist.

sought to broadly understand genetic control of regional pigment loss by examining several breeds with different piebalding patterns. We compared the genomes of piebald and non-piebald pigeons using both genetic crosses and genome-wide association studies, and identified several genetic changes affecting the endothelin receptor gene *EDNRB2*. Our findings highlight how independent mutations at a single locus can drive diversification of plumage pigment patterning within a species.

Introduction

Vertebrates display striking variation in both pigmentation types and patterning. In a natural setting, intraspecific pigment variation is often associated with sexual dimorphism or adaptation to different environmental conditions across a species range. Similarly, selective breeding in domestic species has given rise to a diverse array of pigment patterns [1,2]. Variation in pigment patterns within and among vertebrates reflects underlying changes in cell migration and function that can have profound impacts on health, behavior, and survival [2–5]. Thus, identifying molecular changes that underlie variation in pigment patterning is crucial to understanding both the evolutionary origins of diversity and the etiology of pigment-related developmental disorders.

One broad category of pigment patterning that has evolved repeatedly within and among species is piebalding. Piebald patterns are characterized by patches of pigmented and non-pigmented skin, hair, feathers, or scales. Among mammals, piebalding is linked to multiple pigmentation pathway genes, including *KIT* in horses and pigs, *EDNRB* in horses and mice, and *MITF* in dogs and cattle [6–12]. In addition to altering pigment patterning, genetic variants sometimes have broader pleiotropic effects. For example, disruption of *EDNRB* is associated with enteric nervous system defects, while changes at the *MITF* locus are linked to deafness [5,9,13,14]. Therefore, understanding the genetic and developmental mechanisms that control depigmentation phenotypes has critical relevance from developmental, evolutionary, and clinical perspectives.

Domestic pigeons (*Columba livia*) are an ideal model to study the genetics of plumage depigmentation and piebald patterning. For centuries, hobbyists have selected for a wide range of depigmentation phenotypes, ranging from "recessive white" birds that exhibit total loss of both plumage and iris pigmentation to an array of "piebald" markings, defined as any patchwork of white and colored plumage [15,16]. Some breeds, such as the Helmet, have mostly white plumage with patches of pigmented feathers restricted to the head and tail (Fig 1A). Conversely, other breeds like the Mookee have very little white plumage, limited to the head and the primary flight feathers (Fig 1B). The inheritance patterns of piebalding also vary. Crosses between piebald and non-piebald breeds show that some piebald patterns have dominant inheritance, others are recessive, and some show variability in plumage patterning among F_1 offspring [15]. Based on analyses of phenotypes from a variety of crosses, prior work implies that different genetic factors control piebald patterning in different body regions, and that some combinations of depigmented plumage are caused by multiple linked variants on the same chromosome [15,17].

In this study, we use parallel genetic, genomic, and developmental biology approaches to test these genetic predictions. We previously used quantitative trait locus (QTL) mapping in an F_2 intercross to identify two loci that contribute to piebalding [18]. Here, we evaluate three additional crosses to identify similarities and differences in both phenotypes and the genetic architecture of piebalding in additional breeds. Next, we examine whole genome sequences

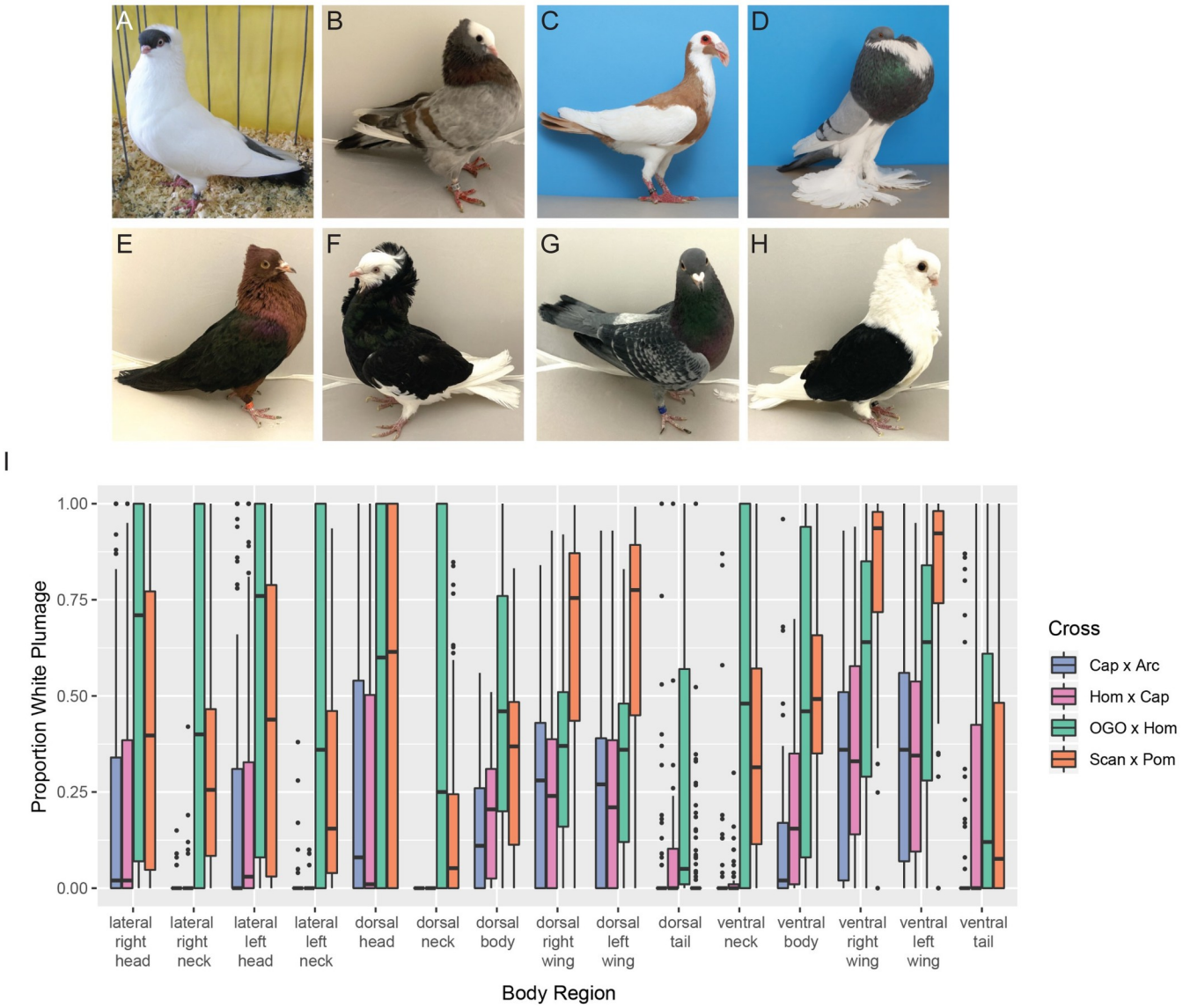

Fig 1. Piebald patterns vary among breeds and within F_2 crosses. (A-H) Examples of piebald and cross founder breeds. (A) Helmet, (B) Mookee, (C) Scandaroon (Scan x Pom founder breed), (D) Pomeranian Pouter (Scan x Pom founder breed), (E) Archangel (Cap x Arc founder breed), (F) Old Dutch Capuchine (Cap x Arc and Hom x Cap founder breed), (G) Racing Homer (Hom x Cap and OGO x Hom founder breed), (H) Old German Owl (OGO x Hom founder breed). E and F are images of founders of the Cap x Arc cross, others are representative images. (I) Boxplots showing the distribution of the proportion of white plumage for F_2 birds from each cross in the 15 different body regions quantified. Boxes span from the first to third quartile of each data set, with lines indicating the median. Whiskers span up to 1.5x the interquartile range. Photos in (C) and (D) by Layne Gardner, used with permission.

https://doi.org/10.1371/journal.pgen.1010880.g001

from a wide array of pigeon breeds to test for associations between genotypes and piebalding phenotypes. Through these complementary approaches, we identify both breed-specific and shared loci associated with piebalding. At a major locus associated with piebalding in multiple breeds, we identify a candidate gene, *EDNRB2*, with a mix of coding, noncoding, and structural variants. Our combined genetic, genomic, and developmental results indicate that multiple variants at the same locus likely produce the diverse suite of phenotypes that breeders have selected under domestication.

Results

Piebald phenotypes vary among laboratory crosses

As a first step in mapping the genetic architecture of piebalding, we examined phenotypes in three F_2 crosses, each with one piebald and one non-piebald founder. The first cross was derived from a piebald female Old Dutch Capuchine and a non-piebald male Archangel (Cap x Arc), the second from a non-piebald female Racing Homer and a piebald male Old Dutch Capuchine (Hom x Cap), and the third from a piebald female Old German Owl and a non-piebald male Racing Homer (OGO x Hom). In addition, we compared these three crosses to a previously analyzed cross derived from two piebald founder breeds, the Scandaroon and the Pomeranian Pouter (Scan x Pom, two female Scan crossed to the same male Pom) [18]. Comparing piebalding in crosses with diverse piebald founders allows us to identify potential differences in the genetic basis of this trait among breeds.

We quantified the proportion of white and pigmented plumage across 15 different body regions in each cross (Fig 1I). For most body regions, we observed overlap in the range of plumage phenotypes observed among crosses; however, we found differences in both the extent and distribution of white plumage in some body regions. Much of this variation is consistent with expectations based on founder phenotypes. For example, in the Cap x Arc and Hom x Cap crosses, we never observed white plumage on the dorsal neck, but fully white dorsal necks are common in the OGO x Hom cross. The Old German Owl founder of the OGO x Hom cross has a fully white neck, while the Old Dutch Capuchines have pigmented dorsal neck plumage and limited white feathering on the ventral and lateral neck. In another example, the extent of white feathering on the wings is greater in the Scan x Pom cross compared to other crosses. Consistent with the wing phenotype of F_2s, the Scandaroon founder breed has a broader region of white plumage on the dorsal wing compared to the Old German Owl or Old Dutch Capuchine (see Fig 1C–1H).

Principal component analysis (PCA) of piebalding phenotypes, measured as the proportion of white plumage in each of 15 body regions, shows overlap in the phenotypic space occupied by all four crosses. One exception is a subset of OGO x Hom F_2 offspring that separate from other pigeons on both PC1 and PC2, which reflect the level of white plumage in different body regions (S1 Fig, blue triangles at lower right). These individuals have more extensive white plumage than the most extreme phenotypes in other crosses, with many closely recapitulating the Old German Owl founder breed (Fig 1H). While variability both within and among crosses aligns well with expectations based on founder phenotypes, the founder phenotypes do not strictly define the limits of piebalding in F_2 birds. Several F_2 individuals have white plumage in body regions where cross founders do not (S2A and S2B Fig), suggesting that either the effects of genetic modifiers not visible in the phenotypes of the founders, stochasticity, or both may play a role in determining the extent of piebalding.

We next sought to determine if piebalding consistently co-occurred in two or more specific body regions in our crosses (S2 Fig), which might suggest shared genetic control of those regions. We found that in the Cap x Arc and Hom x Cap crosses, the strongest correlations are within body regions (e.g., lateral head and dorsal head, dorsal left wing and dorsal right wing), with the head, wing, and tail forming independent "modules" that separate out over PC2. In the OGO x Hom cross, correlation is high across most body regions, and PC2 is primarily defined by tail pigmentation. In the Scan x Pom cross, we identified two sets of correlated regions, one comprising the neck and body and the other comprising the head and the wing. This result is similar to our previous findings for this cross that identified two major QTLs for piebalding, one contributing primarily to white plumage on the ventral neck and dorsal body, and the other contributing to white plumage on the wings and head [18].

In summary, we found inconsistent linkages between piebald body regions among the F_2 progeny of four lab crosses. These patterns could arise from multiple piebalding-associated genetic variants, some of which affect plumage depigmentation in a single body region and some of which drive depigmentation across multiple body regions.

Shared and cross-specific loci control plumage depigmentation

We next asked which regions of the genome affected plumage depigmentation. We used QTL mapping to identify loci associated with the proportion of white plumage across 15 different body regions in the Cap x Arc, Hom x Cap, and OGO x Hom crosses (Figs 2, S3–S5, Table 1). A major-effect QTL on LG15 was associated with piebalding across many body regions in all three new crosses and this locus was also a major-effect QTL in the Scan x Pom cross [18]. Thus, a single locus drives a substantial proportion of the variation in piebald patterning in multiple breeds (Fig 3, Table 1). The boundaries of QTL intervals vary both among crosses and body regions: the union of 2-LOD intervals from the peak marker for all crosses and body regions spans 14.7 Mb and 11 genomic scaffolds of the Cliv_2.1 assembly. However, the intersection of all 2-LOD intervals in all crosses spans only 162 kb on scaffold 507 (NCBI accession AKCR02000023.1) and contains two annotated genes—*RPAC2* and *EDNRB2*—and 128 kb of intergenic space 5' of *EDNRB2*.

While the LG15 QTL is shared between crosses, the Cap x Arc and OGO x Hom crosses also have QTLs associated with piebalding on other linkage groups that are cross-specific, indicating that piebalding phenotypes can be polygenic (Figs 2B, 2E, S3 and S5). The OGO x Hom cross has a second major-effect QTL on LG14 that contributes to piebalding across many body regions (Figs 2E and S5), while the Cap x Arc cross has a minor effect QTL on LG13 that primarily impacts the ventral neck and dorsal body (Figs 2B and S3).

A single genomic locus is consistently associated with piebalding in a wide variety of pigeon breeds

QTL mapping showed that piebalding is controlled by LG15 in several breeds; however, this method could not tell us whether these and other piebald breeds share the same genetic variants in the candidate region. Therefore, we examined allele frequency differentiation between the genomes of piebald (43 genomes, 31 breeds) and non-piebald (98 genomes, 44 breeds and feral pigeons) pigeons using probabilistic F_{ST} (pF_{ST}) [19,20]. We identified a single well-differentiated peak on scaffold 507 that is strongly associated with piebalding (Fig 4A). Overall, 296 SNPs on 14 scaffolds reached the threshold for genome-wide statistical significance. Of these, 265 (90%) are within a 373-kb region spanning scaffold 507:11066907–11440529, and 43 SNPs define a smaller 215-kb region that reaches the maximum pF_{ST} statistic.

The 215-kb region spans three complete genes (*VAMP7*, *RPAC2*, and *EDNRB2*), a portion of a fourth gene (*LOC102097680*, SLAIN motif-containing protein-like), and approximately 140 kb of intergenic space 5' of *EDNRB2*. Therefore, this pF_{ST} candidate region converges on the same region identified by QTL mapping: it lies completely within the broadest interval defined by all four crosses and spans the entirety of the 162-kb minimal candidate QTL interval. Given the association of this region with piebalding in all four crosses and a diverse panel of genomes, we chose to focus on the shared LG15/scaffold 507 candidate interval as the major piebalding candidate region.

Piebald pigeons do not share a single haplotype at the candidate locus

The candidate region on scaffold 507 is associated with piebalding in many breeds. However, the variance in phenotypes and inheritance among crosses raises the possibility of allelic

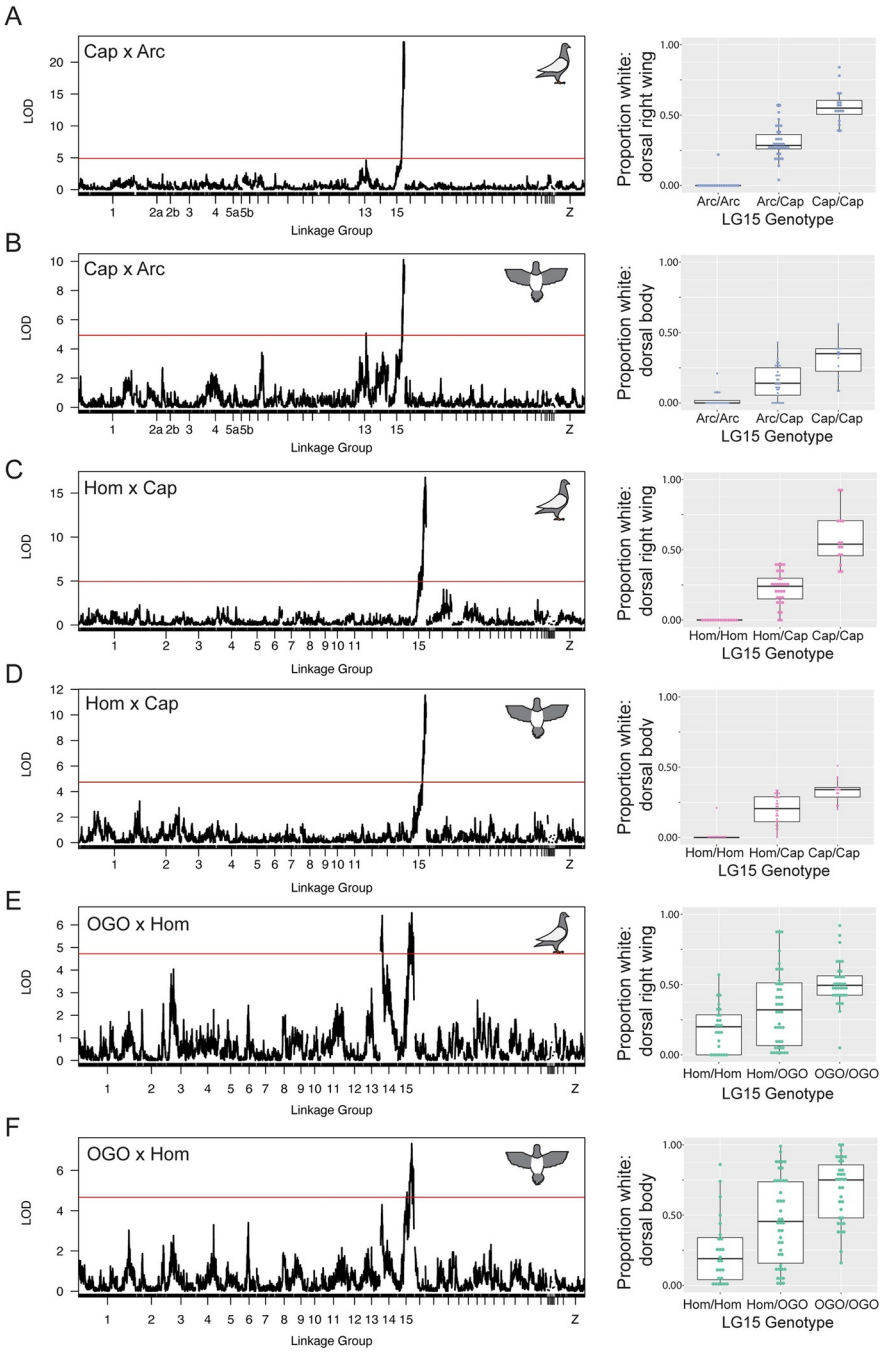

Fig 2. QTL mapping identifies shared and cross-specific regions associated with piebalding. Representative QTL results for piebalding in the Cap x Arc (A-B), Hom x Cap (C-D), and OGO x Hom (E-F) crosses. A,C, and E show QTL results for the dorsal right wing. B, D, and F show QTL results for the dorsal body. Lefthand plots illustrate QTL mapping results, with linkage map position on the X-axis and LOD score on the Y-axis. Red lines indicate the threshold for genome-wide statistical significance. Righthand boxplots illustrate the relationship between genotype at the LG15 peak marker and the proportion of white plumage in that body region. In all boxplots, individuals homozygous for the non-piebald founder allele are on the left and individuals homozygous for the piebald founder allele are on the right. Boxes span from the first to third quartile of each data set, with lines indicating the median. Whiskers span up to 1.5x the interquartile range. QTL mapping results for additional body regions are in S3, S4, and S5 Figs.

https://doi.org/10.1371/journal.pgen.1010880.g002

Table 1. Summary of QTL analysis for regional white plumage in the Cap x Arc, Hom x Cap, and OGO x Hom crosses. PVE, percent variance explained; peak marker given as (scaffold:position).

	Cap x Arc				Hom x Cap				OGO x Hom			
Body Region	**Linkage Group**	**Peak Marker**	**Peak LOD score**	**PVE**	**Linkage Group**	**Peak Marker**	**Peak LOD score**	**PVE**	**Linkage Group**	**Peak Marker**	**Peak LOD score**	**PVE**
Lateral Right Head	15	1916:103567	18.5	70.9	15	507:9653061	20.9	81.1	15	1916:291786	6.5	25.7
Lateral Right Neck	Not significant				Not significant				14	1259: 880682	4.9	16.1
									15	507:11385801	6.6	21.8
Lateral Left Head	15	683.1: 222122	15.4	64.1	15	507:10820150	25.2	86.5	15	1916:291786	6.5	25.7
Lateral Left Neck	Not significant				Not significant				14	1259: 880682	5.9	18.9
									15	507: 11385801	6.3	20.3
Dorsal Head	15	1916:147181	13.8	60.2	15	507:10820150	17.3	74.7	15	1916: 291786	5.1	20.8
Dorsal Neck	No depigmentation in this region				No depigmentation in this region				14	1259: 880682	5.8	18.5
									15	1916:291786	6.2	19.7
Dorsal Body	13	1486: 1732159	5.1	9.1	15	507:11027392	11.5	60.0	15	507:11385801	7.3	28.4
	15	1916:103567	10.1	29.4								
Dorsal Right Wing	15	507:11385801	23.2	79.7	15	507:11027392	16.7	73.6	14	1259: 1259791	6.4	26.0
									15	507:11385801	6.5	26.4
Dorsal Left Wing	13	1486: 1188321	5.48	1.1	15	507:10912510	15.3	70.3	14	1259: 844674	5.5	19.7
	15	507:11385801	24.2	50.6					15	507:11385801	8.1	28.4
Dorsal Tail	Not significant				Not significant				14	1259: 1259791	8.2	27.1
									15	507:9260009	4.8	15.8
Ventral Neck	13	493: 4593712	6.6	50.5	15	683.1: 144415	5.9	37.9	14	1259: 880682	5.9	19.5
	15	507:10316297	5.0	43.5					15	507:11385801	5.7	18.7
Ventral Body	15	683.1_222122	8.7	43.9	15	507:11027392	15.3	70.4	14	1259_747998	4.9	16.6
									15	507:11385801	7.4	25.3
Ventral Right Wing	15	1916:103567	23.9	79.8	15	507:11027392	14.1	67.3	15	507:10611804	7.5	29.1
Ventral Left Wing	13	1486: 1188321	5.2	1.2	15	507:11027392	12.9	64.2	15	507:11385801	7.9	30.3
	15	507:11385801	25.6	53.9								
Ventral Tail	Not significant				15	507:9409137	6.0	38.2	14	1259: 880682	8.6	27.3
									15	507:9260009	4.9	14.9

https://doi.org/10.1371/journal.pgen.1010880.t001

heterogeneity at this locus. We examined sequences in the candidate region and found that, for many of the significant SNPs identified by pF_{ST}, piebald-associated alleles are not shared across all piebald genomes. Instead, we identified four haplotype groups (Groups 1–4, below) with distinct patterns of shared SNP genotypes that correlate with piebalding in specific body regions (Figs 4B and S6).

Group 1 includes pigeons with white necks and bodies, partially- to fully-pigmented heads, and pigmented tails. Wing plumage in this group is variable: all birds have white flight feathers, but wing shield feathers can be pigmented or white (e.g., Fig 1A). Group 2 consists primarily of pouter breeds characterized by pigmented heads, white ventral bodies and wing flights, and a U-shaped "bib" marking across the lateral and ventral neck (e.g., Fig 1D). Group 3 contains a

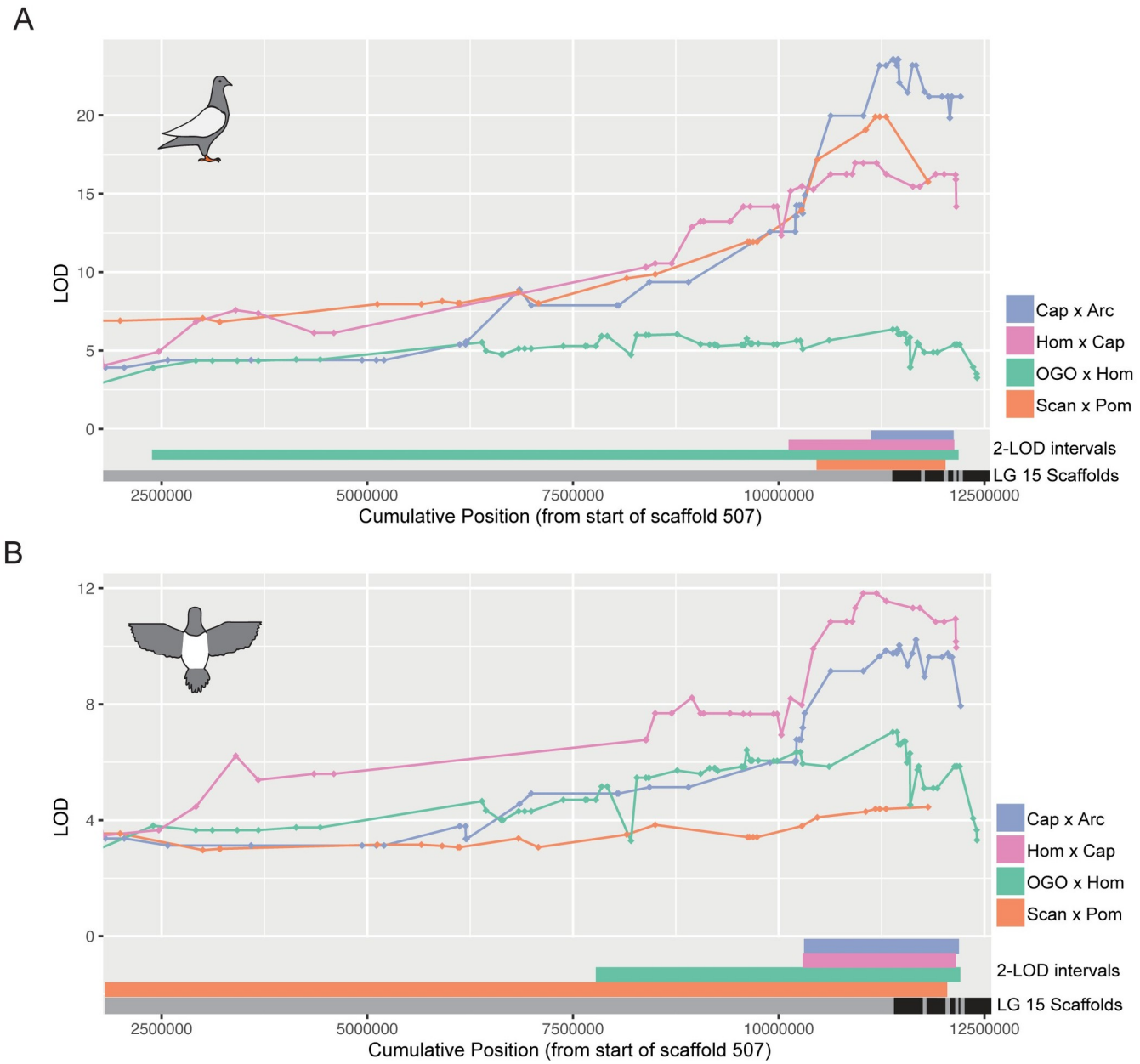

Fig 3. Piebalding QTLs on linkage group 15 overlap in all crosses. Overlaid QTL results for dorsal right wing (A) and dorsal body (B) within the LG15 peak region. 2-LOD intervals for each cross are indicated at the bottom of each plot. Black and gray bars indicate scaffold boundaries for the scaffolds that make up the candidate region in all four crosses; some scaffolds are not represented in all crosses due to lack of informative markers.

https://doi.org/10.1371/journal.pgen.1010880.g003

combination of piebald patterns characterized by white neck and breast plumage and variable piebalding on the head, ranging from patches of white feathers to fully white heads (e.g., Fig 1H). Group 4 consists primarily of birds with patterns that breeders have termed "baldhead" or "monked" (e.g., Fig 1B and 1F). All birds in this group are characterized by primarily white heads and white wing flights. Some also have white wing shields, but the scapular feathers, where the wings articulate with the shoulder, are pigmented (e.g., Fig 1C). Below, we describe the unique genetic signatures at the candidate locus that define each group.

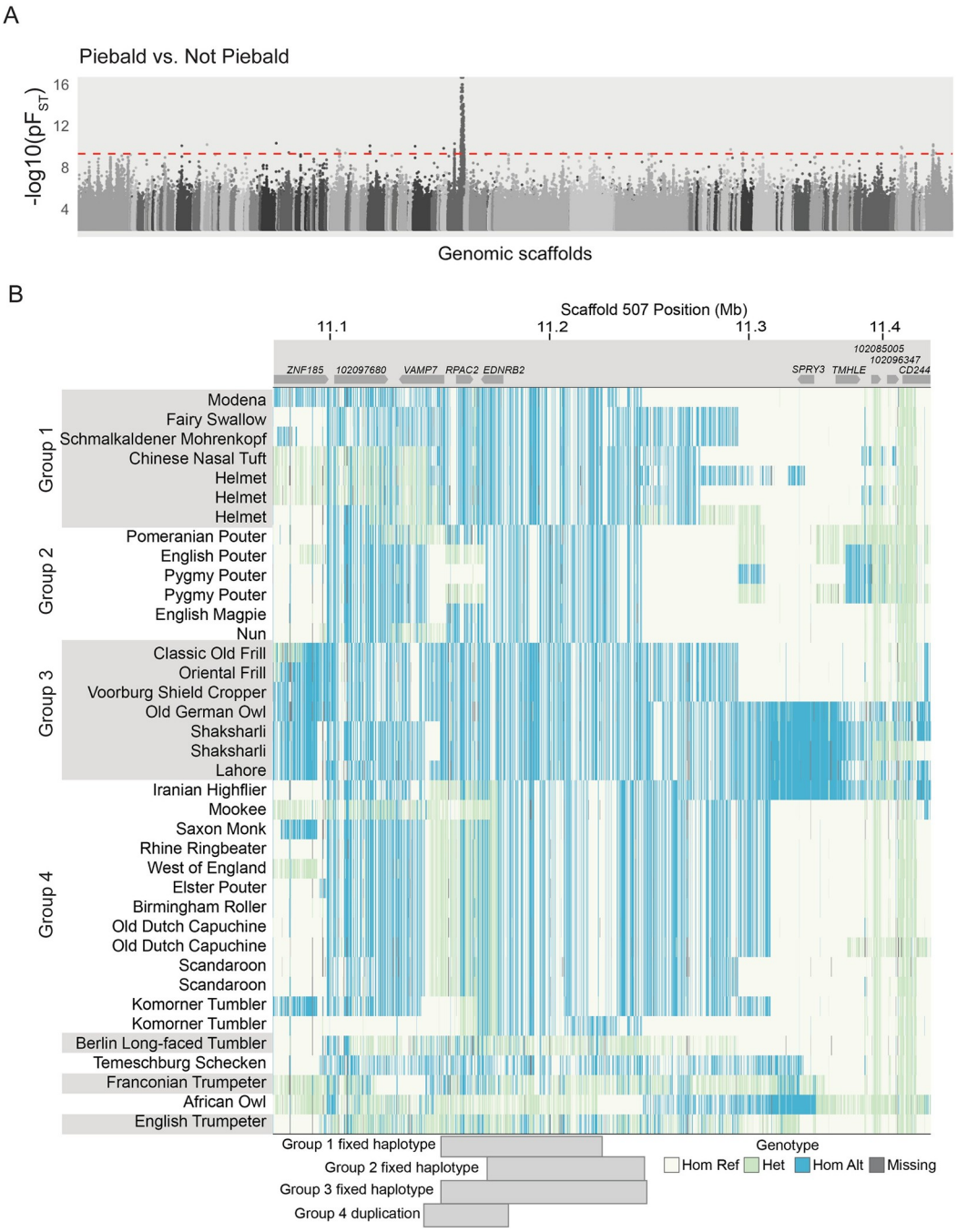

Fig 4. A single genomic locus associated with piebalding across many breeds. (A) Whole-genome pF_{ST} comparisons of piebald birds to non-piebald birds. Dashed red line indicates 5% threshold for genome-wide significance. (B) Plot of genotypes within the candidate region identified by pF_{ST}. Each row shows an individual bird, and each vertical line a SNP position colored by genotype relative to the reference genome. Approximate locations of genes are illustrated at top. Shading on the left-hand side indicates birds with shared fixed haplotypes, the approximate span of these haplotypes is illustrated by gray blocks on the bottom of the plot. Hom Ref, homozygous reference allele; Het, heterozygous; Hom Alt, homozygous alternate (non-reference) allele.

https://doi.org/10.1371/journal.pgen.1010880.g004

Groups 1 and 2: Coding mutations in *EDNRB2* are associated with plumage depigmentation

To assess group-specific allele frequency differentiation, we compared allele frequencies across the scaffold 507 candidate region in each subgroup to non-piebald birds by pF_{ST}. For each group, we first looked for significantly differentiated SNPs, then identified piebald candidate SNPs within the differentiated region. The reference assembly is from a non-piebald bird; therefore, we defined piebald candidate SNPs as variants where the nonreference allele was fixed in the piebald group, but never present in the homozygous state in the non-piebald background genomes.

Group 1: An R290C substitution is associated with piebalding

In Group 1 birds, we identified 31 piebald candidate SNPs spanning 92 kb (scaffold 507: 11137571–11229275) (Fig 5A). A non-reference variant at scaffold 507:11166924 is in exon 5 of *EDNRB2* and, as the only candidate SNP that is located with the coding region, is predicted to cause an amino acid substitution from arginine to cysteine at position 290 (R290C) in the EDNRB2 protein. EDNRB2 is a G-protein coupled receptor with seven transmembrane domains. The R290C substitution lies on the edge of the fifth transmembrane domain and within a putative peptide ligand binding pocket, as predicted based on the structures of ligand-bound family members (accession #cd15977) [21,22]. Protein alignments of the EDNRB2 sequence across five tetrapod species show that the R290 residue is not highly conserved, but this mutation is classified as "probably damaging" by PolyPhen2 (score = 0.981; Fig 5B) [23]. We next screened for this mutation in 47 additional pigeon genomes that were not included in the pF_{ST} analysis and identified one additional bird homozygous for the R290C mutation, an American Highflier. Based on the breed standard, this bird is expected to have a piebalding pattern similar to other birds with the R290C mutation [24].

A E256K mutation in EDNRB2 is linked to recessive white

Our analysis of Group 1 pigeons unexpectedly led to the discovery of a coding mutation associated with a classic pigmentation trait known as "recessive white," which is characterized by completely white plumage and "bull" (dark brown to black) eye color [15]. One of the Group 1 pigeons carrying the R290C mutation belongs to the Modena breed and has piebald markings known as "Gazzi". Extensive crosses by pigeon breeders suggest that Gazzi (z) is allelic and dominant to recessive white (z^{wh}) [15], suggesting that a z^{wh} allele should also be present on a different haplotype at this locus. We examined the *EDNRB2* coding sequence of three bull-eyed white individuals from three different breeds and found a coding mutation in exon 4 (C to T at scaffold 507:11167700). Two of the three birds are homozygous and the third is heterozygous for this nucleotide change, which results in a glutamic acid to lysine substitution in at position 256 (E256K) of the EDNRB2 protein. Like the R290C mutation identified in Group 1 piebald birds, the E256K substitution is predicted to be "probably damaging" to the peptide ligand binding pocket (PolyPhen2 score = 0.999) [23] (Fig 5B). Unlike R290, however, E256 is highly conserved across vertebrates. In addition to its conservation in vertebrate EDNRB2 proteins, this residue is conserved in *C. livia* EDNRB1 and *M. musculus* EDNRB, suggesting it may be critical for the function of endothelin receptors broadly.

To increase our sample size, we used PCR to test for the candidate z^{wh} mutation in 9 additional bull-eyed white pigeons from 7 different breeds. Of these, 6 were homozygous for the E256K mutation, 2 were heterozygous, and 1 did not carry the mutation. These results suggest that the E256K mutation is associated with bull eye color and white plumage, but it is not the

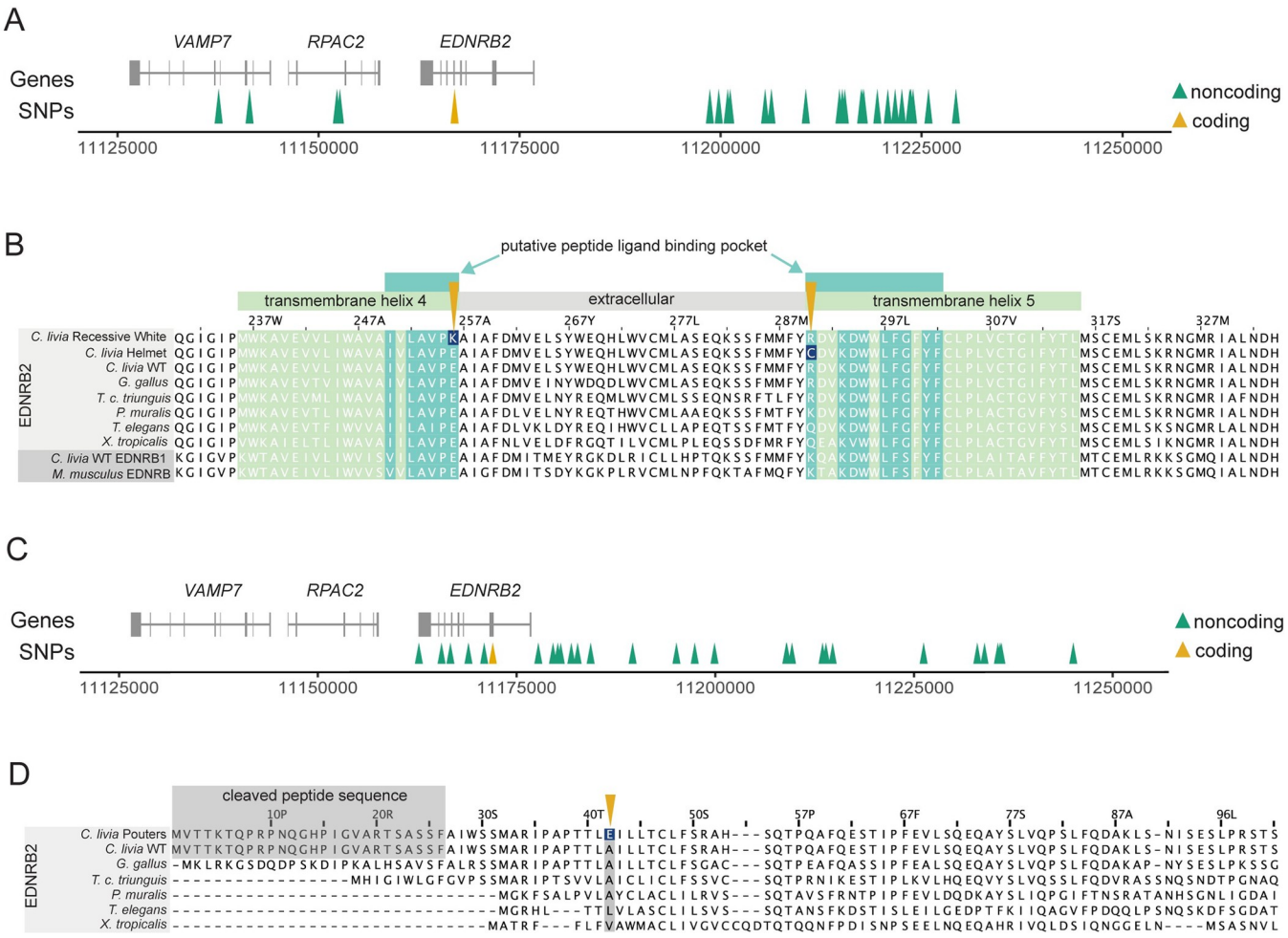

Fig 5. Three coding mutations are associated with plumage depigmentation. (A) Genomic context of the Group 1 piebald haplotype. Gene models for the region are shown in gray. Arrowheads indicate coding (yellow) and non-coding (green) SNPs. (B) Multi-species alignment of a portion of EDNRB2 (light gray rows) and EDNRB/EDNRB1 (dark gray, bottom two rows) protein sequences. Amino acids within a transmembrane helix are shaded in light green, residues that are part of a putative ligand binding pocket are shaded dark green. The coding changes identified in recessive white and Group 1 piebald birds, like the Helmet breed, are marked by yellow arrows, with the altered residues shaded dark blue. (C) Genomic context of the Group 2 piebald haplotype. (D) Multi-species alignment of a portion of EDNRB2 protein sequences. The cleaved peptide at the 5' end of the *C. livia* protein is marked in gray; this portion exists in other species but is not easily delineated in this alignment due to variability of the amino end of the protein. The coding change identified in Group 2 birds is marked a yellow arrow, with the altered residue shaded dark blue.

https://doi.org/10.1371/journal.pgen.1010880.g005

only genetic variant that can cause the bull-eyed white phenotype. In bull-eyed white birds heterozygous for the E256K mutation, genetic background or the presence of other piebalding alleles may contribute to the phenotype. Indeed, through crosses, pigeon breeders have determined that while the recessive white phenotype is common, bull eye color and fully white plumage can also arise from other combinations of alleles, including combinations of multiple piebalding alleles [15].

Group 2: An A42E substitution in EDNRB2 is associated with piebalding

In Group 2 pigeons, we identified 33 piebald candidate SNPs spanning 82 kb (scaffold 507: 11162719–11245041) (Figs 4B and 5C). Only one of these Group 2 variants is a coding variant, which results in an alanine to glutamic acid substitution at position 42 (A42E) of the EDNRB2 protein (Fig 5C). This region is predicted to be an extracellular domain between the signal

peptide sequence and the first transmembrane domain, and multi-species alignments show partial conservation of this residue (Fig 5D). This mutation is classified as "possibly damaging" (PolyPhen2 score = 0.86) [23].

In summary, we identified three coding mutations associated with piebalding in *EDNRB2*. Two are associated with the location and extent of piebalding in Group 1 and 2 pigeons that retain some pigmented plumage, and the third is associated with total loss of plumage pigment in recessive white birds. Two of these coding mutations, E256K and R290C, are in the same ligand binding pocket of the EDNRB2 protein but have markedly different effects on plumage phenotype. Based on amino acid characteristics, conservation of the mutated residues, and the phenotypes of birds harboring these mutations, we hypothesize that the E256K mutation in recessive white birds may create a null allele that disrupts pigment cell precursors throughout the embryo in the homozygous state. In contrast, the R290C mutation in Group 1 piebald birds may create a hypomorphic allele of EDNRB2 with altered binding affinity, leading to partial loss of pigment. These pigeons do not show total loss of plumage pigment, indicating that some level of function is retained. The A42E mutation identified in Group 2 birds does not impact the predicted ligand binding pocket and is associated with the least severe plumage depigmentation phenotype.

Group 3: A putative regulatory change at the *EDNRB2* locus is associated with piebalding

In pigeons from Group 3, which includes both predominantly white "shield marked" breeds like the Old German Owl founder of the OGO x Hom cross and other piebald birds with less extensive white plumage, we identified 33 piebalding candidate SNPs spanning 105 kb (scaffold 507: 11145063–11249818) (Figs 4B and 6A). We observed extended shared homozygous haplotypes in subsets of Group 3 birds, but opted not to evaluate these regions further as both small sample size and the interrelatedness of breeds in this group would make it difficult to rule out population stratification as a driver of differentiation.

Of the 33 piebalding candidate SNPs in Group 3, one was a coding SNP in exon 4 of *EDNRB2*. This coding mutation is synonymous and thus not likely to impact EDNRB2 function. We next examined the remaining 32 fixed noncoding SNPs to identify putative regulatory variants. We aligned genomic sequence from pigeon to orthologous regions in 15 other avian species and 6 non-avian species to identify evolutionarily conserved noncoding elements among birds and tetrapods, respectively. We defined conserved noncoding elements (CNEs) as regions with >70% sequence identity in 10 or more avian species (avian CNEs) or 3 or more non-avian tetrapods (tetrapod CNEs) [25]. We identified 9 SNPs in avian CNEs, 3 of which also overlap with tetrapod CNEs (Fig 6A). Five of these SNPs were predicted to result in loss of one or more transcription factor binding sites [26]. One SNP in a CNE conserved in 14 of 15 avian species is predicted to result in loss of an XBP1 binding site upstream of *EDNRB2*. This is particularly relevant to piebalding as *XBP1* is linked to pigment loss as a candidate gene for vitiligo in humans, and loss of a predicted XBP1 binding site near *EDNRB2* is associated with plumage depigmentation in ducks [27,28]. Based on these findings, we hypothesized that the Group 3 haplotype includes regulatory variants that could cause plumage depigmentation by impacting the expression of *EDNRB2* or other candidate region genes.

To test this hypothesis, we examined expression of candidate genes by RNA-seq in OGO x Hom F_2 individuals (n = 6). We separately sequenced mRNA from white and pigmented regenerating feather buds from adult birds and performed differential expression analysis to quantify changes in gene expression between pigmented and non-pigmented feather buds. This F_2 cross was founded by an Old German Owl, a representative breed from Group 3, and

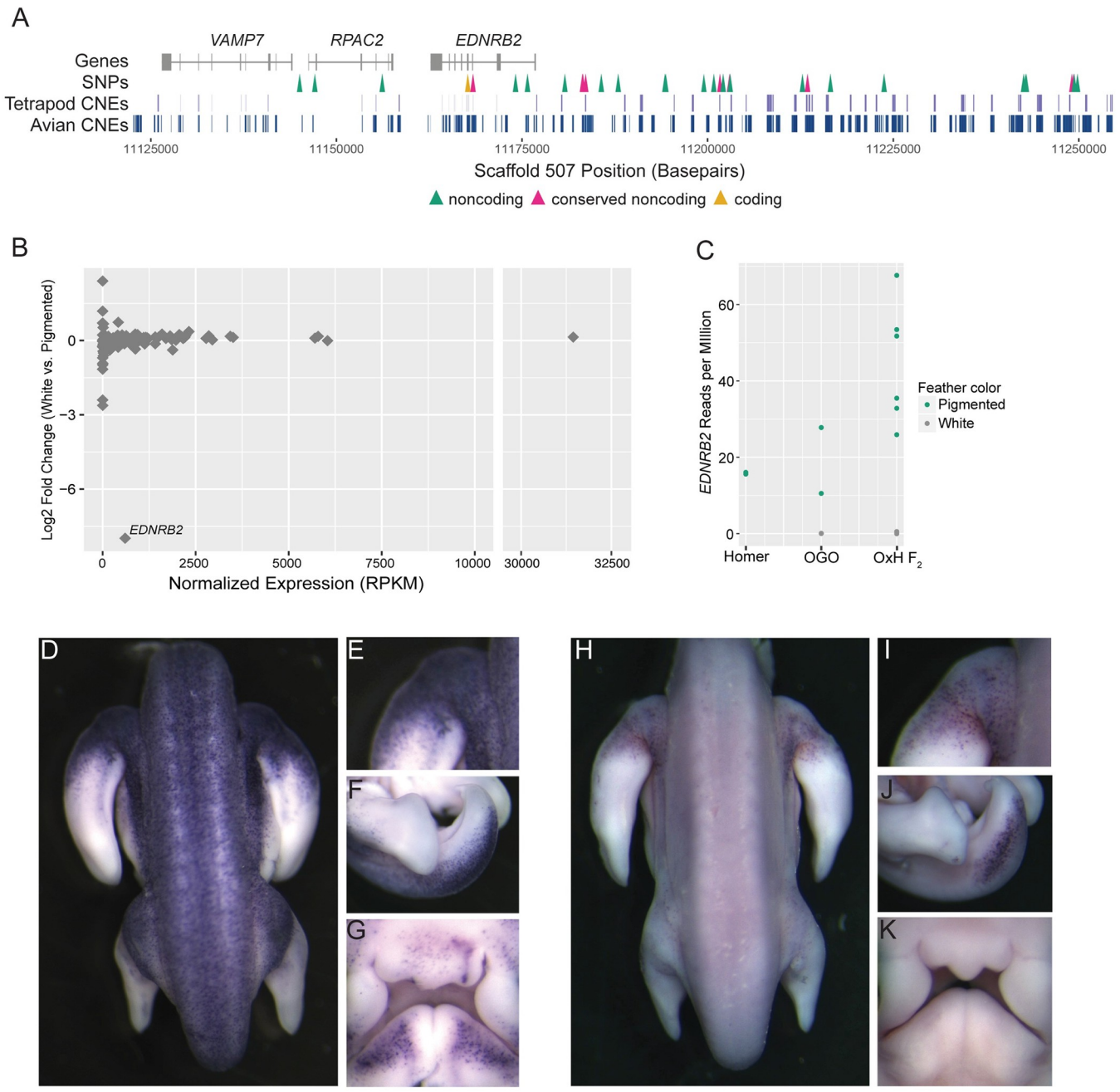

Fig 6. *EDNRB2* expression is altered in piebald birds. (A) Genomic context of the Group 3 piebald haplotype. Gene models for the region are shown in gray. Arrowheads denote SNPs in the following regions: yellow, coding regions; pink, non-coding regions that overlap with conserved non-coding elements; green, other noncoding regions. Conserved noncoding elements (CNEs) from tetrapod (upper) and avian-only (lower) alignments are shown in blue. (B) Differential expression (by RNA-seq) of genes within the OGO x Hom LG15 candidate region comparing white vs. pigmented regenerating feather buds from OGO x Hom F_2 pigeons. One gene, *EDNRB2* is significantly downregulated in white feather buds. (C) Normalized *EDNRB2* read count from RNA-seq in adult Racing Homers (pigmented feather buds only), Old German Owls (OGO, pigmented and white feather buds), and OGO x Hom F_2s (OxH F_2, pigmented and white feather buds). (D-K) Whole-mount *in situ* hybridization for *EDNRB2* in Racing Homer (D-G) and Classic Old Frill (H-K) embryos. Panels show dorsal body (D,H), Proximal forelimb (E,I), tail (F,J), and facial primordia (G,K).

https://doi.org/10.1371/journal.pgen.1010880.g006

piebald F_2 birds are expected to carry the Group 3 haplotype at the LG15 locus. While the fixed SNPs shared by Group 3 birds delineate a narrow candidate region spanning portions of three genes, we took a conservative approach and quantified gene expression across the broader

LG15 candidate region identified by the OGO x Hom QTL analysis, which includes 112 genes. We found that only one gene within the LG15 candidate region, *EDNRB2*, was significantly differentially expressed (Fig 6B and 6C). *EDNRB2* was expressed in collar cells from pigmented feather buds but was absent in collar cells from white feather buds.

We next evaluated RNA-seq from the founder Racing Homer (non-piebald, n = 2) and Old German Owl (piebald, n = 2) breeds. Consistent with the results from OGO x Hom F_2 feather buds, *EDNRB2* is expressed in pigmented Racing Homer and Old German Owl feather buds, but not in white Old German Owl feather buds (Fig 6C); only pigmented feather buds were sampled from Racing Homers as no white feathers are present in non-piebald birds. While the level of *EDNRB2* expression in pigmented regenerating feather buds varies between individuals, our RNA-seq analyses establish that *EDNRB2* expression is lost in the white feather buds of piebald birds, while other genes in the LG15 QTL candidate region are not significantly altered. This suggests that one or more of the putative regulatory mutations in Group 3 gives rise to changes in *EDNRB2* expression associated with regional plumage depigmentation.

Group 3 piebald embryos show reduction and spatial restriction of *EDNRB2*-positive cells

Our RNA-seq analyses established that *EDNRB2* is differentially expressed between white and pigmented regenerating feather buds of adult birds. One of the primary roles of *EDNRB2* is mediating pigment cell migration and proliferation during embryogenesis. Therefore, we used *in situ* hybridization to examine *EDNRB2* expression in non-piebald Racing Homer embryos and piebald Classic Old Frill (Group 3) embryos across developmental stages that include pigment cell migration (Figs 6D–6K and S7). Classic Old Frills have a piebalding pattern characterized by white heads, bodies, and wing flight feathers, but pigmented wing shields and tails.

We found that piebald embryos show a reduction in both the number and spatial distribution of *EDNRB2*-positive cells, particularly in body regions that are unpigmented in adults. By the equivalent of chicken stage 29 of development [29], *EDNRB2*-positive cells are present throughout the dorsal body, limbs, tail, and face in non-piebald Racing Homer embryos (Fig 6D–6G). In contrast, stage-matched Classic Old Frills have fewer *EDNRB2*-positive cells, and these cells are restricted primarily to the forelimbs and tail bud, the two regions that show pigmented plumage in adults of this breed (Fig 6H–6J). *EDNRB2* positive cells are largely absent from the dorsal body and face (Fig 6H and 6K), which are unpigmented in adults. These expression differences between breeds indicate that piebald patterns are likely established, in part, by altering pigment cell migration and proliferation early in development, both processes in which *EDNRB2* plays a key role [30–32].

We also examined embryonic *EDNRB2* expression in OGO x Hom F_2 embryos. We found extensive variability in both the number and distribution of *EDNRB2*-positive cells, consistent with diverse plumage patterns in the adult F_2 population used for QTL mapping (S7 Fig). In OGO x Hom F_2 embryos, *EDNRB2* expression is consistent with genotype at the LG15 QTL: embryos homozygous for the Racing Homer allele (N = 3) look more like wild-type Racing Homer embryos, while embryos homozygous for the Old German Owl founder allele (N = 3) look more like the embryos of the piebald Classic Old Frill (a close relative of the Old German Owl [33]; both breeds are part of piebalding Group 3). Heterozygous embryos (N = 4) have a range of intermediate phenotypes.

Group 4: A structural variant is associated with "baldhead" piebalding

We next evaluated piebalding candidate SNPs in Group 4, which consists of pigeon breeds with white ("bald") heads. We identified 448 significantly differentiated SNPs on scaffold 507

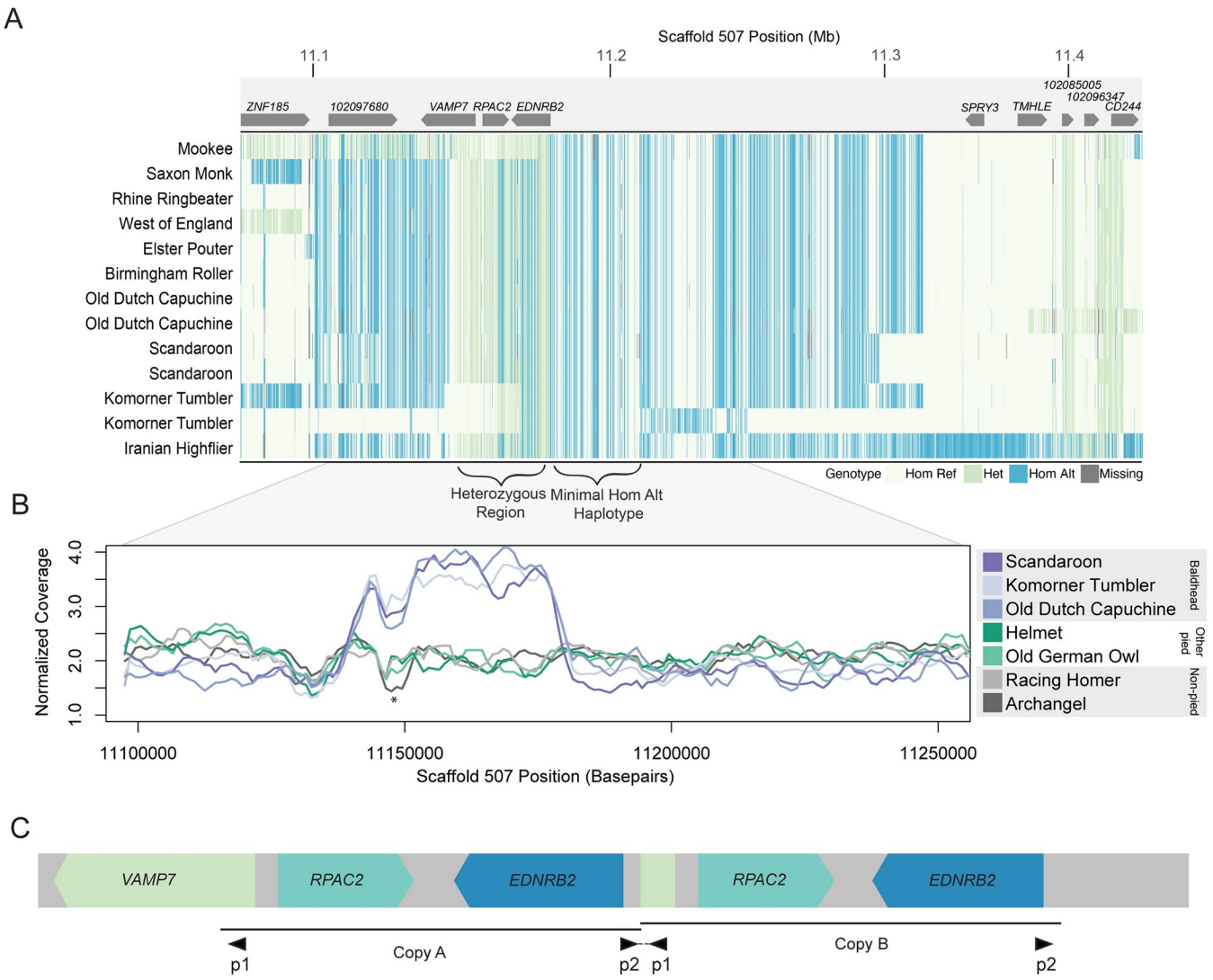

Fig 7. A 37-kb tandem duplication is associated with the Group 4 "baldhead" piebalding pattern. (A) Plot of genotypes within the candidate region identified by pF_{ST} for Group 4 birds. Each row shows an individual bird, and each vertical line a SNP, colored by genotype relative to the reference genome. Approximate locations of genes are illustrated at top, and regions of interest delineated by brackets, below. (B) Plot of normalized whole genome sequencing read coverage for representative birds from seven different breeds. Three baldhead breeds show an increase in coverage. * marks a coverage drop that coincides with both a LINE element and a nearby stretch of "N" bases in the reference genome and is not associated with a piebalding phenotype. (C) Schematic of the predicted structure of the baldhead-associated duplication. The duplicated region includes the 5' portion of *VAMP7* and the entirety of both *RPAC2* and *EDNRB2*. Black triangles below indicate primer pairs used to amplify across the central breakpoint (also see S8 Fig).

https://doi.org/10.1371/journal.pgen.1010880.g007

spanning 619 kb, and the non-reference allele was fixed in baldhead birds at 105 of these positions. However, pigeons homozygous for all piebald-associated non-reference alleles were present in the background set, so homozygosity for these fixed variants was not exclusive to Group 4. In addition to the haplotype enriched in baldhead birds, we noted a region where birds in this group had a large number of heterozygous SNP genotypes and increased sequencing coverage (Fig 7A and 7B). Sequencing reads that align across breakpoints and targeted PCR (S8 Fig) indicate that these birds carry a tandem duplication of a 37-kb region spanning from intron 1 of *VAMP7* to just 5' of *EDNRB2* (Fig 7C).

As our other SNP analyses did not assess structural variation, we screened for the 37-kb duplication in the genomes of 130 non-piebald and piebald pigeons from Groups 1–3 to see if

it was associated with the Group 4 baldhead phenotype or present in non-baldhead individuals. We found two birds heterozygous and two homozygous for the duplication, but one of these homozygotes does not have a baldhead-like piebalding phenotype, suggesting that the duplication itself may not cause the characteristic Group 4 piebalding phenotype.

We did not identify any fixed coding or noncoding piebald-specific candidate SNPs in Group 4 birds. However, the presence of the tandem duplication can hinder accurate variant calling from whole genome sequencing, and variants called as heterozygous may in fact be copy-specific SNPs. Therefore, we turned to RNA-seq data from regenerating feather buds to evaluate expression of genes within the duplicated region, which could reveal regulatory variation. We first examined RNA-seq data from regenerating feather bud collar cells for two representative breeds from Group 4 that carry the duplication, the Old Dutch Capuchine and the Komorner Tumbler. Surprisingly, we found that, unlike Group 3 pigeons, *EDNRB2* is expressed in both white and pigmented regenerating feathers. However, we noted that expression in white regenerating feather buds appeared to be allele specific (S8 Fig). Due to the duplication in this region and the high level of homozygosity at SNPs outside the duplication, we hypothesized that this expression pattern represented differential regulation of the two copies of *EDNRB2* on the same chromosome. By examining variants in reference-mapped RNA-seq data, we identified copy-specific polymorphisms that differentiate the copy of *EDNRB2* expressed in both white and pigmented feathers from the copy expressed only in pigmented feathers.

Feather buds expressing only one copy of *EDNRB2* lack pigment, suggesting that this copy is nonfunctional. This copy has four coding SNPs: three are synonymous substitutions in the white-expressed copy, and the fourth results in a proline to leucine substitution (P434L) that is not predicted to be damaging. Based on these results, coding mutations are unlikely to result in loss of function of the white-expressed *EDNRB2* copy. We next generated *de novo* transcriptome assemblies to look for potential alternative isoforms or fusion transcripts that may lack wild-type function, and identified an *RPAC2/EDNRB2* fusion transcript assembled in Old Dutch Capuchine and Komorner Tumbler *de novo* transcriptomes (baldhead Group 4 breeds), but not in Racing Homer (non-piebald) or Old German Owl (Group 3) *de novo* assemblies. RT-PCR and sequencing confirmed this fusion transcript in white feather buds from Old Dutch Capuchines and Komorner Tumblers (S8 Fig). The predicted fusion transcript from *de novo* assemblies does not include exon 8 of *EDNRB2* and shows intronic read-through of intron 7. However, we also were able to amplify *EDNRB2* transcripts that are properly spliced across this region and include the entire coding portion of exon 8 in white feather buds from Old Dutch Capuchine and Komorner Tumblers, suggesting the presence of multiple white-expressed *EDNRB2* transcripts (S8 Fig). While we are unable to pinpoint the precise structure of all transcripts or their potential functionality, feather buds expressing only one copy of *EDNRB2* lack pigment, indicating that the other variant or fusion transcripts lack wild-type function. Additionally, the restricted expression of the wild-type non-fusion *EDNRB2* transcript in only pigmented feather buds suggests there are unidentified regulatory changes affecting the functional copy.

Discussion

Coding and non-coding mutations in *EDNRB2* are associated with piebalding

Piebalding is a genetically and phenotypically complex suite of depigmentation phenotypes that occurs across many breeds of domestic pigeons. Our QTL mapping studies identify at least four loci that contribute to piebald patterning. Three of these are specific to different

crosses, while one locus on LG15 is a major QTL for piebalding in all crosses, indicating that complex piebald patterns are determined by a combination of breed-specific and shared genetic loci (Fig 2, S2–S5 Figs and Table 1). Among different crosses, the piebald body regions associated with the LG15 QTL are not always the same. For example, LG15 is associated with white plumage on the dorsal and lateral neck in the OGO x Hom cross, but not in the Cap x Arc or Hom x Cap crosses.

Within the shared candidate region, all piebald birds do not share a single haplotype. Instead, we identified multiple haplotypes enriched in, or specific to, subgroups of piebald birds. While the piebald-associated variants differ among groups, all likely alter the expression or function of a single candidate gene, *EDNRB2*. We identified a mix of coding variants, a putative cis-regulatory variant, and a structural variant at this locus, indicating that multiple classes of genetic change at a single locus likely contribute to diverse piebalding patterns in pigeons.

While some of the diversity of piebalding patterns is likely driven by a series of *EDNRB2* alleles, many pigeons sharing the same *EDNRB2* mutation show differences in pigment pattern. For example, pigeons homozygous for the R290C mutation in *EDNRB2* typically have pigmented heads and tails and white bodies, but pigment on the wing shield varies. Likewise, Group 3 birds carrying the same putative regulatory SNP show variation in tail pigmentation. This is consistent with the presence of additional piebalding-associated QTLs in three of our crosses. We propose that the extensive diversity of piebald patterns across domestic pigeons is controlled by the combination of *EDNRB2* allelic heterogeneity and interacting breed-specific modifiers, whose molecular identities remain unknown. Future work will further evaluate the contributions of cross-specific modifiers from QTLs on LG13 (Cap x Arc cross), LG14 (OGO x Hom), and LG1 (Scan x Pom).

Multiple biological mechanisms could give rise to regionalized depigmentation

The establishment of epidermal pigment patterning is a complex process. Epidermal pigment cells are neural crest-derived, and multiple mechanisms can contribute to pigment loss, including defects in cell migration, proliferation, differentiation, function, and survival [4,34,35]. Upregulation of *EDNRB2* is required for pigment cell precursors to enter the dorsolateral migration pathway, mediated in part by a chemotactic response to the *EDN3* ligand [30,36]. *EDN3* also promotes melanoblast proliferation, drives ectodermal invasion, and promotes differentiation, indicating that *EDNRB2* is critical for all these processes [32,37,38]. Thus, any changes in *EDNRB2* expression or function could result in global or local plumage depigmentation.

The *EDNRB2* haplotypes we identified are associated with an array of depigmentation phenotypes. The most severe phenotype, recessive white, is associated with a protein coding change at a highly conserved residue within the putative ligand binding pocket of EDNRB2. Pigeons homozygous for this mutation lack plumage pigment and have bull eyes. Pigeon breeders have long noted an association between white plumage and bull eyes, and we previously mapped bull eye color to the *EDNRB2* locus [18]. Bull eyes appear dark due to a loss of two types of pigment in the iris stroma, allowing the dark retinal pigment epithelium at the back of the eye to show through [39]. Epidermal and iris stromal pigment are neural crest-derived, while the retinal pigment epithelium is not. Total loss of epidermal and iris stromal pigment could arise from failure of neural crest cells to enter the dorsolateral migration pathway or from widespread failure of melanoblast survival and differentiation. Future work examining expression of *EDNRB2* and other melanoblast markers in recessive white embryos could distinguish between these possibilities.

While the recessive white mutation ablates all epidermal pigmentation, a major question that arises from our study of piebald pigeons is how regionally restricted changes in depigmentation are established. For example, we found coding mutations associated with regional effects on plumage pigment, such as the *EDNRB2* R290C substitution in Group 1 birds. This could arise from a combination of changes in ligand-receptor binding affinity and non-uniform expression of ligand throughout the developing embryo, altering local interaction dynamics between piebald-associated EDNRB2 variants and the EDN3 ligand. Such changes could impact many facets of pigment patterning, including migration, proliferation, invasion, or differentiation of pigment cells. Future assessment of *EDN3* expression and the quantity and distribution of *EDNRB2*-positive cells in birds harboring the R290C mutation could determine if one or all of these processes are affected.

We also identified haplotypes at the *EDNRB2* locus that are not expected to impact protein function. Instead, Group 3 piebald pigeons share a putative regulatory mutation within an evolutionarily conserved noncoding element 5' of *EDNRB2*, which could affect pigment patterning by altering the timing, location, or level of *EDNRB2* expression. Changes in the timing or level of *EDNRB2* expression caused by regulatory mutations could impact both number and spatial distribution of migrating melanoblasts or mature melanocytes. In mice, *KIT*, not *EDNRB*, regulates melanoblast migration and differentiation. Experiments examining the effects of c-KIT inhibition in developing mouse embryos shows differentiation is spatially non-uniform, and disrupting KIT at different times leads to spatially distinct depigmentation patterns [40]. Temporally specific changes in *EDNRB2* expression could produce similar outcomes in some piebald pigeons. As *EDNRB2* plays key roles in migration, proliferation, and differentiation, other mechanisms could also give rise to breed specific patterns. For example, the specific *EDNRB2* expression pattern observed in Classic Old Frill embryos might arise from decreased proliferation coupled with a chemotactic response to long-range cues, such as EDN3 or Fibroblast Growth Factors, resulting in a reduced number of pigment cells accumulating in specific body regions [30,41].

Endothelin B signaling mutations are associated with depigmentation in other vertebrates

Endothelin signaling is linked to changes in pigment patterning in numerous vertebrate species. Among birds, for example, tyrosinase-independent mottling in chickens, "spot" plumage in ducks, and "panda" plumage in quail are all associated with identical, convergently evolved substitutions in the sixth transmembrane domain of EDNRB2 [42–44]. Another coding mutation, in the extracellular loop between the fourth and fifth transmembrane domains, is associated with predominantly white plumage and dark eyes in Minohiki chickens [44]. This mutation does not result in fully white feathers (some dark spots persist), but like the recessive white mutation in pigeons, it impacts both plumage and iris color.

Recurrent mutations in the endothelin signaling pathway associated with pigmentation changes are not limited to birds. For example, a recent study identified an allelic series at the *EDNRB2* locus associated with distinct color morphs in ball pythons [45,46]. Zebrafish do not have a syntenic *EDNRB2* ortholog, but *EDNRBA* is critical for pigment cell migration and maturation [47]: an allelic series at the "rose" locus (*EDNRBA)* produces a range of pigmentation phenotypes, and includes missense, nonsense, and uncharacterized mutations [48]. Given the repeated involvement of *EDNRB2* in piebalding in genetically tractable domestic species, this gene should also be considered a viable candidate for pigment pattern variation among wild species. Plumage patterns featuring depigmented patches are common in myriad wild bird species, including magpies, from which the term "piebald" is derived: "pie" references the

magpie's black-and-white plumage, and "bald" refers to white patches or streaks, as in the white head plumage of the bald eagle.

Pleiotropy may constrain or permit the generation of allelic series

Endothelin pathway mutations are well documented in mammals, and they are often associated with pleiotropic effects. The endothelin signaling pathway evolved through multiple rounds of gene duplication, and expression of different combinations of endothelin receptors and ligands characterize unique cell populations [49]. In therian mammals, one endothelin B receptor copy was lost, and a single endothelin B receptor, *EDNRB*, remains. In humans, mice, and horses, *EDNRB* mutations are associated with changes in pigmentation but are coupled with deleterious effects on enteric nervous system development [9,10,14,50]. The allelic series associated with piebalding in pigeons likely would not have arisen without subfunctionalization of *EDNRB1* and *EDNRB2* that uncouples pigment patterning from enteric nervous system development. More broadly, the retention of *EDNRB2* in birds may have been crucial for the evolution of the diverse, heritable piebalding patterns of domestic pigeons, ducks, chickens, and quail.

Like *EDNRB2*, mutations in *MC1R* and *TYRP1* that alter pigmentation are also common across species [51–59]. In both cases, there are limited pleiotropic effects, though some *TYRP1* mutations in mice are associated with progressive hearing loss related to melanocyte degeneration and *MC1R* mutations are associated with altered immune response and analgesia [60,61]. Some *TYRP1* mutations may even confer a selective advantage, as seen in the "cinnamon" morph of American black bears [53].

The subfunctionalization of *EDNRB2* in non-mammalian vertebrates–and the developmentally-restricted functions of other pigment genes like *TYRP1* –may permit pigment diversification more readily than other traits. Interestingly, analysis of teleost fish genomes suggests that pigment genes may have been preferentially retained following genome duplication, and that this may have been a driving force behind the diversification of teleost pigment types and patterns [62]. Whole genome duplications provide the opportunity for subfunctionalization or neofunctionalization of duplicated genes while limiting the negative impacts of pleiotropy. This suggests that lack of pleiotropy may be a driving force in pigment diversification across both domestic and wild species [2,63,64].

Multiple mechanisms may drive repeated mutation at the *EDNRB2* locus

EDNRB2 may be a repeated mutational target in avians for a variety of reasons. Not only are pigment patterns highly visible and readily subject to selection, but subfunctionalization of the two *EDNRB* paralogs in avians also limits the pleiotropic effects of *EDNRB2* mutations. This allows for mutations to persist in populations and may provide a larger effective mutational target: coding changes, *cis*-regulatory changes, and structural variants are all potentially survivable or advantageous. In genes with multiple critical roles in development, *cis*-regulatory variants are common as altering modular regulatory elements can circumvent deleterious pleiotropic effects [63].

In some cases, the sequence content of genes or their regulatory regions can also mediate repeated mutation [65,66]. A preliminary evaluation of the *EDNRB2* region in the Cliv_2.1 assembly reveals an enrichment of both annotated transposable elements and assembly gaps (typically indicative of repetitive sequence) that may make this region more prone to mutation (S9 Fig). Future work examining *EDNRB2* in wild avian species could determine whether convergent mutations are found across species and whether the same suite of pigment genes that drive intraspecific variation in domestic pigeons, chickens, quail, and ducks also impact interspecific variation in wild species.

Materials and methods

Ethics statement

Animal husbandry and experimental procedures were performed in accordance with protocols approved by the University of Utah Institutional Animal Care and Use Committee (protocols 10–05007, 13–04012, 19–02011, and 22–03002).

Phenotyping of F_2 offspring

Four intercrosses were used in these studies. An intercross between a male Archangel and a female Old Dutch Capuchine generated 98 F_2 offspring [18]. An intercross between a female Racing Homer and a male Old Dutch Capuchine generated 82 offspring. An intercross between a male Racing Homer and a female old German Owl generated 171 F_2 offspring [67]. An intercross between a male Pomeranian Pouter and two female Scandaroons generated 131 F_2 offspring [68].

Whole genome resequencing

DNA was extracted from blood samples collected with breeders' written permission at the annual Utah Premier Pigeon Show or from our lab colony using the Qiagen DNEasy Blood and Tissue Kit (Qiagen, Valencia, CA). Samples were treated with RNAse during extraction. Isolated DNA was submitted to the University of Utah High Throughput Genomics Shared Resource for library preparation using the Illumina Tru-Seq PCR-Free library kit. The resulting libraries were sequenced on either the Illumina HiSeq or Illumina NovaSeq platforms. Raw sequence data for thirteen previously unpublished samples are available in the NCBI Sequence Read Archive under BioProject accession PRJNA986561. These data sets were combined with previously published data sets (BioProject accessions PRJNA513877, PRJNA428271, and PRJNA167554, PRJNA680754) for variant calling.

Genomic analyses

Variant calling was performed with FastQForward, which wraps the BWA short read aligner and Sentieon (sentieon.com) variant calling tools to generate aligned BAM files (fastq2bam) and variant calls in VCF format (bam2gvcf). Sentieon is a commercialized variant calling pipeline that allows users to follow GATK best practices using the Sentieon version of each tool [69]. FastQForward manages distribution of the workload to these tools on a compute cluster to allow for faster data-processing than when calling these tools directly, resulting in runtimes as low as a few minutes per sample.

A step-by-step summary of the workflow is available at support.sentieon.com/manual/DNAseq_usage/dnaseq/. Briefly, Raw sequencing reads from resequenced individuals were aligned to the Cliv_2.1 reference assembly [70] using fastq2bam, which utilizes the default settings of the BWA aligner. Reads are then de-duplicated using samblaster. Variant calling was performed on 199 resequenced individuals, including 186 previously published samples [67,68,71–73], using bam2gvcf with the quality filter "--min_base_qual 20", and individual genome variant call format (gVCF) files were created. Joint variant calling was performed on all 199 individuals using the Sentieon GVCFtyper algorithm.

The subsequent variant call format (VCF) file was used for pF_{ST} analysis using the GPAT+ + toolkit within the VCFLIB software library (https://github.com/vcflib). pF_{ST} uses a probabilistic approach to detect differences in allele frequencies between populations using a modified likelihood ratio test that incorporates genotype likelihood information [19,74]. For piebald vs. non-piebald pF_{ST} analysis, the genomes of 43 piebald birds from 31 breeds were compared to

the genomes of 98 non-piebald birds (44 breeds and feral pigeons). Three breeds had both piebald and non-piebald representatives included in the analysis. The threshold for genome-wide significance was determined by Bonferroni correction (a threshold of 0.05 / total number of SNPs assayed).

Plumage phenotyping

Individual birds from F_2 crosses were quantitatively phenotyped. Following euthanasia, photos were taken of F_2 plumage including dorsal and ventral views with wings and tail spread, and lateral views with wings folded. We divided the body into 15 different regions for phenotyping: dorsal head, right lateral head, left lateral head, dorsal neck, ventral neck, right lateral neck, left lateral neck, dorsal body, ventral body, dorsal tail, ventral tail, dorsal right wing, dorsal left wing, ventral right wing, and ventral left wing. To score each region, we imported photos into Photoshop v21.1.0x64 (Adobe, San Jose, CA) and used the magic wand tool to select only the white feathers within the body region. Following this selection, we saved two separate images: one containing the entire region (both pigmented and white feathers) with the color for the white feathers inverted (hereafter, "whole region image"), and one with the selected white feathers removed and only the pigmented feathers remaining ("pigmented region image"). For each body region, we imported these two images into ImageJ (v1.52a; [75] and converted them to greyscale, then used the threshold tool to measure the number of pixels in each image. To calculate the proportion of white feathers for each region, we subtracted the number of pixels in the pigmented region image from the number of pixels in the whole region image, then divided by the number of pixels in the whole region image. See S1 Table for phenotype data. Principal component analysis (PCA) of plumage phenotypes was performed in R (v3.6.3) [76] using the *prcomp* function, with the proportion of white plumage in each of the 15 body regions scored used as input.

Samples used for pF_{ST} were qualitatively scored as "piebald" or "non-piebald" from photographs, with published breed standards used as a reference for expectations. Birds with fully white plumage or unclear phenotyping photographs were excluded from pF_{ST} analysis, as were birds with white plumage only on the flight feathers, since breeders classify white flights as a separate phenotype unrelated to piebalding.

Genotype-by-sequencing

DNA samples from founders of the crosses and their F_2 progeny were extracted using the Qiagen DNeasy Blood and Tissue kit. Our genotype-by-sequencing (GBS) approach was adapted from a previously published protocol with minor modifications [68,77]. DNA was digested with ApeKI, and size selected for fragments in the 550–650 bp range. Domyan et al. (2016) performed an initial round of genotyping for the Pomeranian Pouter x Scandaroon cross. These libraries were sequenced using 100- or 125 bp paired-end sequencing on the Illumina HiSeq2000 platform at the University of Utah Genomics Core Facility. Genotype by sequencing for the Archangel x Capuchine founders (n = 2) and F_2 offspring (n = 98), Homer x Capuchine founders (n = 2) and F2 offspring (n = 82), and Homer x Old German Owl founders (n = 2) and F_2 offspring (n = 171), as well as supplemental sequencing for 20 additional and 17 previously low-coverage Pomeranian Pouter x Scandaroon F_2s, was performed by the University of Minnesota Genomics Center. New GBS libraries were sequenced on a NovaSeq 1x100 SP flow cell.

Linkage map construction

GBS reads were trimmed using CutAdapt [78], then mapped to the Cliv_2.1 reference genome reads using Bowtie2 [79]. Genotypes were called using Stacks2 by running "refmap.pl" [80].

We constructed genetic maps using R/qtl v1.46–2 (www.rqtl.org) [81]. Autosomal markers showing significant segregation distortion ($p < 0.01$ divided by the total number of markers genotyped, to correct for multiple testing) were eliminated. Sex-linked scaffolds were assembled and ordered separately, due to differences in segregation pattern for the Z chromosome. Z-linked scaffolds were identified by assessing sequence similarity and gene content between pigeon scaffolds and the Z chromosome of the annotated chicken genome (Ensembl Gallus_gallus-5.0).

Pairwise recombination frequencies were calculated for all autosomal and Z-linked markers. Markers with identical genotyping information were identified using the "findDupMarkers" command, and all but one marker in each set of duplicates was removed. Within individual Cliv_2.1 scaffolds, markers were filtered by genotyping rate; to retain the maximal number of scaffolds in the final map, an initial round of filtering was performed to remove markers where fewer than 50% of birds were genotyped. Large scaffolds (> 40 markers) were subsequently filtered a second time to remove markers where fewer than 66% of birds were genotyped.

Within individual scaffolds, R/Qtl functions "droponemarker" and "calc.errorlod" were used to assess genotyping error. Markers were removed if dropping the marker led to an increased LOD score, or if removing a non-terminal marker led to a decrease in length of >10 cM that was not supported by physical distance. Individual genotypes were removed if they had error LOD scores >5 (a measure of the probability of genotyping error, see [82]. Linkage groups were assembled from both autosomal markers and Z-linked markers using the parameters (max.rf 0.15, min.lod 6). Scaffolds in the same linkage group were manually ordered based on calculated recombination fractions and LOD scores. Linkage groups in the Pomeranian Pouter x Scandaroon map were numbered by marker number. Linkage groups in the Archangel x Old Dutch Capuchine, Homer x Old Dutch Capuchine, and Homer x Old German Owl maps were numbered based on scaffold content to correspond with Pomeranian Pouter x Scandaroon linkage groups.

Quantitative trait locus mapping

We performed QTL mapping using R/qtl v1.46–2 [81]. We used the *scanone* function to perform a single-QTL genome scan using Haley-Knott regression. For each phenotype, the 5% genome-wide significance threshold was calculated by running the same *scanone* with 1000 permutation replicates. For each significant QTL peak, we calculated 2-LOD support intervals using the *lodint* function. We calculated percent variance explained (PVE) using the *fitqtl* function.

Identification of evolutionarily conserved non-coding regions

We identified syntenic regions spanning *ZNF185* to *TMHLE* in fifteen avian species (*Athene cunicularia*, *Anas platyrhynchos*, *Calypte anna*, *Corvus brachyrhynchos*, *Cuculus canorus*, *Coturnix japonica*, *Falco peregrinus*, *Gallus gallus*, *Haliaeetus leucocephalus*, *Hirundo rustica*, *Manacus vittelinus*, *Nipponia nippon*, *Pygoscelis adeliae*, *Struthio camelus*, and *Taeniopygia guttata*) and six non-avian tetrapods (*Alligator mississippiensis*, *Chrysemys picta bellii*, *Crocodylus porosus*, *Podarcis muralis*, *Thamnophis elegans*, and *Xenopus tropicalis*) using NCBI ortholog annotations and genome browser records. This region contains *EDNRB2* and its 5' intergenic space, and encompasses the entire candidate region identified by pF_{ST}. We pulled FASTA sequence from the syntenic region from the NCBI genome browser for each species and aligned these sequencing using mVISTA [25]. We defined a conserved non-coding element as any region at least 100 bp in length conserved with >70% sequence identity in 10 or more

avian species (avian CNEs) or 3 or more non-avian tetrapods (tetrapod CNEs) that do not overlap annotated exons.

Evolutionarily conserved regions containing SNPs were identified by comparing the coordinates of significant SNPs fixed in Group 3 birds to tetrapod and avian CNE intervals. We generated FASTA files for CNE intervals containing both the reference and non-reference alleles using the bedtools *getfasta* function (v. 2.28.0) [83], and used TransFac Match 1.0 (http://gene-regulation.com/cgi-bin/pub/programs/match/bin/match.cgi) [26] to predict transcription factor binding sites separately for reference allele CNE sequence and alternate allele CNE sequence. We then compared lists of predicted transcription factor binding sites to identify predicted binding motifs that are gained or lost in Group 3 birds.

Collection of collar cells from regenerating feather buds

Collar cells were collected as described previously [71]. Briefly, secondary covert wing feathers were plucked to stimulate regeneration and allowed to regenerate for 9 days. After nine days, regenerating feather buds were plucked and the proximal 5 mm was cut, bisected, and stored in RNA later at 4˚C overnight. Feather buds were dissected and collar cells removed; cells were then stored at -80˚C until RNA isolation.

Expression analysis from RNA-seq data

RNA from the collar cells of regenerating feather buds was isolated using the Qiagen RNEasy Kit (Qiagen, Valencia CA), treated with the Zymo PCR Inhibitor Removal kit (Zymo Research, Irvine CA) to remove melanin, and submitted to the University of Utah High Throughput Genomics Shared Resource for Illumina TruSeq stranded library preparation. Libraries were sequenced on the Illumina NovaSeq platform. Data are available in NCBI Sequence Read Archive under BioProject PRJNA986561.

We mapped reads to the Cliv_2.1 reference genome using STAR [84], and counted reads in features using FeatureCounts [85]. We assessed differential expression in OGO x Hom F_2 samples with DESeq2 [86]. Due to the small sample size for each breed-specific sample, we did not perform differential expression analysis. For genes of interest, we calculated and plotted normalized gene expression based on the number of uniquely mapped reads within the gene model and the total number of reads per sample.

Protein conservation, structure prediction, and mutation evaluation

We obtained protein sequences for EDNRB2 orthologues across species using NCBI blastp and generated multi-species alignments using Clustal Omega [87], and then visualized using Jalview2 [88]. The boundaries of conserved domains were determined from the NCBI Conserved Domain Database for protein accession number cd15977 (https://www.ncbi.nlm.nih.gov/Structure/cdd/cddsrv.cgi?uid=320643, last access date 8/17/2022) [21,22]. The probable impact of coding mutations were evaluated using the PolyPhen2 web server (http://genetics.bwh.harvard.edu/pph2/, access date 8/17/2022) [23].

Identification and evaluation of structural variants

We identified reads with aberrant insert sizes within the scaffold 507 candidate region using both the Samtools suite and visualization with the IGV genome browser [89,90]. In a subset of samples, we observed large pileups of read pairs with larger than normal insert sizes at two loci, within *VAMP7* and upstream of *EDNRB2*, and an apparent increase in coverage between them. We also identified numerous soft-clipped reads within *VAMP7* and directly upstream of

EDNRB2 and used NCBI BLAST to compare this soft-clipped sequence to the Cliv_2.1 reference genome [70,91]. Mapping of this soft-clipped sequence suggested a tandem duplication. We next calculated coverage across 5 kb sliding windows on scaffold 507 using the Bedtools *genomecov* function (v2.28.0) [83]. Coverage was normalized to 2x and plotted. We designed primers near the predicted duplication breakpoints (Left `TATGCAGCAGCACACAAACA`; Right `GCAGTCACTCGTTTCCCTCT`) and used PCR to amplify across the central breakpoint of the tandem duplication to confirm its presence.

De novo transcriptome assembly and analysis

Transcriptomes were assembled from collar cell RNAseq data using Trinity v. 2.11.0 with the "—jaccard-clip" option [92]. Transcripts fully or partially matching *EDNRB2* were identified by NCBI Blast [91], using the *de novo* transcriptome assembly as the database. These transcripts were then aligned to the reference *EDNRB2* mRNA sequence (accession XM_021292346.1) using Clustal Omega [93]. Portions of assembled transcripts that did not align to *EDNRB2* mRNA were compared to the Cliv_2.1 reference genome and transcriptome using NCBI Blast to evaluate sequence similarity to intronic and intergenic sequence as well as other annotated genes. The predicted fusion transcript between *EDNRB2* and *RPAC2* was then validated by RT-PCR.

RT-PCR

RNA from collar cells was isolated as for RNA-seq. cDNA was synthesized from isolated collar cell RNA using the Invitrogen SuperScript IV first strand synthesis system and Oligo dT primer (Invitrogen #18091050). We then used this cDNA as input for PCR. *EDNRB2* expression was assessed using a reverse primer in *EDNRB2* exon 8 (`CCCCAGGTTATGTTGGTCAC`) and a forward primer in *EDNRB2* exon 7 (`CCCTGTGGCTCTCTACTTCG`). The presence of an RPAC2/EDNRB2 fusion transcript was confirmed using a reverse primer in *EDNRB2* (3' to 5' in exon 2 of *EDNRB2;* `GCCAAGCTAGCAATGAGGAC`*)* and forward primer in *RPAC2* (3' to 5' in intron 1 of *RPAC2*; `GGGTTGCAACATCTGCACTA`).

In situ hybrization

ISH probe templates were generated by PCR amplification using primers targeting a portion of pigeon *EDNRB2* (279-bp amplicon, Fwd ATGAGGAGGAGAGGGAGAGG; Rev AAGGTGAAGAGAAGGGGTGG) from a cDNA library generated from pooled feather bud samples from multiple breeds. *The EDNRB2* amplicon were cloned into pGEM-T Easy (Promega) and confirmed by Sanger sequencing. To generate sense and antisense probes, pGEM-*EDNRB2* was digested with NcoI and transcribed with SP6 RNA polymerase (sense) or digested with SalI and transcribed with T7 RNA polymerase (antisense).

Racing Homer, Classic Old Frill, and OGO x Hom F_2 embryos used for ISH were dissected from eggs at the desired embryonic stage and fixed overnight in 4% paraformaldehyde at 4˚C on a shaking table. Embryos were subsequently dehydrated into 100% MeOH and stored at −20˚C. Whole-mount ISH was performed essentially as previously described following a protocol optimized for avian embryos (http://geisha.arizona.edu/geisha/protocols.jsp) [67].

Repeat, transposable element, and N tract quantification

Intervals annotated as simple repeats or transposable elements were extracted from the Cliv_2.1 repeat annotation GFF [70]. Locations of N tracts were extracted in BED format using perl. Random windows size-matched to the candidate region across scaffold 507 were

generated using the bedtools (v. 2.8.2) *random* function, and overlap of windows with repeats, TEs, and N tracts calculated using bedtools *intersect* [83].

Supporting information

S1 Fig. Principal Component Analysis of piebalding within F_2 crosses. Principal component analysis of plumage phenotyping data for 15 different body regions (shown in Fig 1I) for each cross. Points represent individual F_2 birds and are colored by cross.
(TIF)

S2 Fig. Quantification of plumage depigmentation in F_2 crosses. (A) Representative Old German Owl (OGO x Hom founder breed) piebalding phenotype, showing pigmented feathers on the entire wing shield and alula. (B) An example F_2 bird from the OGO x Hom cross showing depigmentation on the wing shield that is more extensive than the founder Old German Owl phenotype seen in (A). (C-F) Principal component analysis (left) and correlation diagrams (right) examining relationships between pigmentation across body regions. Arrows show PCA loadings indicating the relative contributions of white plumage in each body region to PC1 and PC2. DT, dorsal tail. DN, dorsal neck. DB, dorsal body. VB, ventral body. LLN, lateral left neck. LRN, lateral right neck. VN, ventral neck. VLW, ventral left wing. VRW, ventral right wing. VT, ventral tail. DH, dorsal head. DLW, dorsal left wing. DRW, dorsal right wing. LRH, lateral right head. LLH, lateral left head.
(TIF)

S3 Fig. QTL mapping identifies loci associated with piebalding in the Cap x Arc cross. X axis shows linkage groups, Y axis shows LOD score. Red lines indicate the threshold for genome-wide statistical significance. The dorsal neck region was not analyzed in this cross as no F_2 birds showed depigmentation in this area.
(TIF)

S4 Fig. QTL mapping identifies loci associated with piebalding in the Hom x Cap cross. X axis shows linkage groups, Y axis shows LOD score. Red lines indicate the threshold for genome-wide statistical significance. The dorsal neck region was not analyzed in this cross as no F_2 birds showed depigmentation in this area.
(TIF)

S5 Fig. QTL mapping identifies loci associated with piebalding in the OGO x Hom cross. X axis shows linkage groups, Y axis shows LOD score. Red lines indicate the threshold for genome-wide statistical significance.
(TIF)

S6 Fig. Piebald birds share several distinct haplotypes within the scaffold 507 candidate region. Plot of genotypes within the candidate region identified by pF_{ST}. Each row shows an individual bird, and each vertical line a SNP, colored by genotype in relation to the reference genome. Samples are clustered by principal component analysis of genotypes. Samples highlighted in purple are piebald individuals, all others are non-piebald. Hom Ref, homozygous reference allele; Het, heterozygous; Hom Alt, homozygous alternate (non-reference) allele.
(TIF)

S7 Fig. *In situ* hybridization for *EDNRB2* shows changes in number and distribution of *EDNRB2* positive cells between non-piebald and piebald birds. (A,B) Dorsal body of Hamburger-Hamilton stage 24 (HH24) non-piebald Homer (A) and piebald Classic Old Frill (B).

(C-H) HH32 non-piebald Homer (C,E) and piebald Classic Old Frill (D,F). C-D, Dorsal body. Insets show the regions indicated by the white squares. E-F, tail bud. (G-J) *in situ* hybridization for *EDNRB2* in representative HH28 Old German Owl x Homer F_2 embryos. Genotypes for the peak LG15 QTL marker were determined by Sanger Sequencing and are shown below each embryo.
(TIF)

S8 Fig. Allele-specific expression of an *EDNRB2* fusion transcript in piebald birds with the baldhead-associated duplication. (A) example showing coverage of DNA sequencing (top) and RNA sequencing (middle and bottom) in samples from a representative Old Dutch Capuchine at the *EDNRB2* locus. Introns (line) and exons (block) are diagrammed in blue below. Yellow arrows mark two informative SNP sites within *EDNRB2* exons. At these sites, colored bars indicate the proportion of reference (orange and red, respectively) or nonreference (green) allele in aligned reads. DNA sequencing indicates that this individual is heterozygous at both sites. RNA-seq from pigmented feathers shows that both alleles are expressed. RNA-seq from white feathers shows expression of only the nonreference (green) allele. Colored bars not marked with arrows are additional SNPs that are not informative for allele-specific expression due to homozygosity or location outside of *EDNRB2* exons. (B) Schematic of the predicted structure of the baldhead-associated duplication. The duplicated region includes the 5' portion of *VAMP7* and the entirety of both *RPAC2* and *EDNRB2*. Black triangles below indicate locations of primers. (C) PCR of duplication breakpoint using primers P1 and P2. RH, Racing Homer. OGO, Old German Owl. Cap, Old Dutch Capuchine. Scan, Scandaroon. KT, Komorner Tumbler. (D) RT-PCR using primers P3 and P4 confirms the presence of an *RPAC2/ EDNRB2* fusion transcript in white and pigmented feathers from Group 4 Old Dutch Capuchines and Komorner Tumblers, but not other breeds. P, pigmented feather bud sample; W, white feather bud sample. (E) RT-PCR for *EDRNB2* confirms the presence of transcripts spliced across exons 7 and 8 in all samples except white feather buds from Old German Owls.
(TIF)

S9 Fig. The *EDNRB2* candidate region is enriched for N tracts and transposable elements. (A) Schematic of the 373 kb piebalding region identified by pF_{ST} (See Fig 4). Scaffold position is indicated on the X axis. Gray boxes show approximate locations of genes. The locations of transposable elements (TEs), satellite and simple repeats, low complexity regions, and N tracts are indicated below gene models. (B) Boxplots quantifying coverage by N tracts (left) simple repeats (middle) and transposable elements (right), as annotated by RepeatMasker in the candidate region (pink) and 50 random size-matched regions on scaffold 507 (gray and blue). Blue dots indicate randomly generated regions that partially overlap the candidate region; gray indicates regions with no overlap. Boxes span from the first to third quartile of each data set, with lines indicating the median. Whiskers span up to 1.5x the interquartile range, points beyond whiskers are outliers.
(TIF)

S1 Table. Plumage phenotyping data for all crosses.
(XLSX)

Acknowledgments

We thank current and former members of the Shapiro lab for assistance with sample collection and processing. We thank Anna Vickrey, Hannah van Hollebeke, and Alexa Davis for technical assistance and advice. Support and resources from the Center for High Performance

Computing at the University of Utah are gratefully acknowledged. Layne Gardner generously shared the Pomeranian Pouter and Scandaroon photographs in Fig 1. We thank members of the Utah Pigeon Club for providing samples.

Author Contributions

Conceptualization: Emily T. Maclary, Michael D. Shapiro.

Data curation: Emily T. Maclary, Elena F. Boer, Atoosa M. Samani.

Formal analysis: Emily T. Maclary, Ryan Wauer, Bridget Phillips, Audrey Brown, Elena F. Boer, Atoosa M. Samani.

Funding acquisition: Michael D. Shapiro.

Investigation: Emily T. Maclary, Ryan Wauer, Bridget Phillips, Audrey Brown.

Methodology: Emily T. Maclary, Michael D. Shapiro.

Project administration: Michael D. Shapiro.

Resources: Michael D. Shapiro.

Supervision: Emily T. Maclary, Michael D. Shapiro.

Visualization: Emily T. Maclary.

Writing – original draft: Emily T. Maclary, Michael D. Shapiro.

Writing – review & editing: Emily T. Maclary, Ryan Wauer, Bridget Phillips, Audrey Brown, Elena F. Boer, Atoosa M. Samani, Michael D. Shapiro.

References

1. Cieslak M, Reissmann M, Hofreiter M, Ludwig A. Colours of domestication. Biol Rev. 2011; 86: 885–899. https://doi.org/10.1111/j.1469-185X.2011.00177.x PMID: 21443614
2. Hubbard JK, Uy JAC, Hauber ME, Hoekstra HE, Safran RJ. Vertebrate pigmentation: from underlying genes to adaptive function. Trends Genetics Tig. 2010; 26: 231–9. https://doi.org/10.1016/j.tig.2010.02.002 PMID: 20381892
3. Price AC, Weadick CJ, Shim J, Rodd FH. Pigments, Patterns, and Fish Behavior. Zebrafish. 2008; 5: 297–307. https://doi.org/10.1089/zeb.2008.0551 PMID: 19133828
4. Kelsh RN, Harris ML, Colanesi S, Erickson CA. Stripes and belly-spots—a review of pigment cell morphogenesis in vertebrates. Semin Cell Dev Biol. 2008; 20: 90–104. https://doi.org/10.1016/j.semcdb.2008.10.001 PMID: 18977309
5. Reissmann M, Ludwig A. Pleiotropic effects of coat colour-associated mutations in humans, mice and other mammals. Semin Cell Dev Biol. 2013; 24: 576–586. https://doi.org/10.1016/j.semcdb.2013.03.014 PMID: 23583561
6. Karlsson EK, Baranowska I, Wade CM, Hillbertz NHCS, Zody MC, Anderson N, et al. Efficient mapping of mendelian traits in dogs through genome-wide association. Nat Genet. 2007; 39: 1321–1328. https://doi.org/10.1038/ng.2007.10 PMID: 17906626
7. Hofstetter S, Seefried F, Häfliger IM, Jagannathan V, Leeb T, Drögemüller C. A non-coding regulatory variant in the 5′-region of the MITF gene is associated with white-spotted coat in Brown Swiss cattle. Anim Genet. 2019; 50: 27–32. https://doi.org/10.1111/age.12751 PMID: 30506810
8. Brooks SA, Lear TL, Adelson DL, Bailey E. A chromosome inversion near the KIT gene and the Tobiano spotting pattern in horses. Cytogenet Genome Res. 2008; 119: 225–230. https://doi.org/10.1159/000112065 PMID: 18253033
9. Metallinos DL, Bowling AT, Rine J. A missense mutation in the endothelin-B receptor gene is associated with Lethal White Foal Syndrome: an equine version of Hirschsprung Disease. Mamm Genome. 1998; 9: 426–431. https://doi.org/10.1007/s003359900790 PMID: 9585428

10. Koide T, Moriwaki K, Uchida K, Mita A, Sagai T, Yonekawa H, et al. A new inbred strain JF1 established from Japanese fancy mouse carrying the classic piebald allele. Mamm Genome. 1998; 9: 15–19. https://doi.org/10.1007/s003359900672 PMID: 9434939

11. Giuffra E, Törnsten A, Marklund S, Bongcam-Rudloff E, Chardon P, Kijas JMH, et al. A large duplication associated with dominant white color in pigs originated by homologous recombination between LINE elements flanking KIT. Mamm Genome. 2002; 13: 569–577. https://doi.org/10.1007/s00335-002-2184-5 PMID: 12420135

12. Rubin C-J, Megens H-J, Barrio AM, Maqbool K, Sayyab S, Schwochow D, et al. Strong signatures of selection in the domestic pig genome. Proc National Acad Sci. 2012; 109: 19529–19536. https://doi.org/10.1073/pnas.1217149109 PMID: 23151514

13. Stritzel S, Wöhlke A, Distl O. A role of the microphthalmia-associated transcription factor in congenital sensorineural deafness and eye pigmentation in Dalmatian dogs. J Anim Breed Genet. 2009; 126: 59–62. https://doi.org/10.1111/j.1439-0388.2008.00761.x PMID: 19207931

14. Issa S, Bondurand N, Faubert E, Poisson S, Lecerf L, Nitschke P, et al. EDNRB mutations cause Waardenburg syndrome type II in the heterozygous state. Hum Mutat. 2017; 38: 581–593. https://doi.org/10.1002/humu.23206 PMID: 28236341

15. Sell A. Pigeon Genetics. Sell Publishing. Verlag Karin und A. Sell; 2012.

16. Levi W. The Pigeon. ed 2. Revised. Sumter, S.C.: Levi Publishing Co., Inc; 1986.

17. Christie W, Wriedt C. Die Vererbung von Zeichnungen, Farben und anderen Charakteren bei Tauben. Zeitschrift Für Induktive Abstammungs- Und Vererbungslehre. 1924; 32: 233–298. https://doi.org/10.1007/bf01816754

18. Maclary ET, Phillips B, Wauer R, Boer EF, Bruders R, Gilvarry T, et al. Two Genomic Loci Control Three Eye Colors in the Domestic Pigeon (Columba livia). Mol Biol Evol. 2021;38: msab260-. https://doi.org/10.1093/molbev/msab260 PMID: 34459920

19. Kronenberg Z. GENOTYPE-PHENOTYPE ASSOCIATION USING HIGH THROUGHPUT SEQUENCING DATA. Doctoral Dissertation. J. Willard Marriott Digital Library, University of Utah. 2015. https://collections.lib.utah.edu/ark:/87278/s6dg18z9

20. Garrison E, Kronenberg ZN, Dawson ET, Pedersen BS, Prins P. A spectrum of free software tools for processing the VCF variant call format: vcflib, bio-vcf, cyvcf2, hts-nim and slivar. PLoS Comput Biol. 2022; 18: e1009123. https://doi.org/10.1371/journal.pcbi.1009123 PMID: 35639788

21. Lu S, Wang J, Chitsaz F, Derbyshire MK, Geer RC, Gonzales NR, et al. CDD/SPARCLE: the conserved domain database in 2020. Nucleic Acids Res. 2019; 48: D265–D268. https://doi.org/10.1093/nar/gkz991 PMID: 31777944

22. Marchler-Bauer A, Lu S, Anderson JB, Chitsaz F, Derbyshire MK, DeWeese-Scott C, et al. CDD: a Conserved Domain Database for the functional annotation of proteins. Nucleic Acids Res. 2011; 39: D225–D229. https://doi.org/10.1093/nar/gkq1189 PMID: 21109532

23. Adzhubei I, Jordan DM, Sunyaev SR. Predicting Functional Effect of Human Missense Mutations Using PolyPhen-2. Curr Protoc Hum Genetics. 2013; 76: 7.20.1–7.20.41. https://doi.org/10.1002/0471142905.hg0720s76 PMID: 23315928

24. National Pigeon Association. National Pigeon Association Book of Standards. Goodlettsville, TN: Purebred Pigeon Publishing; 2010.

25. Frazer KA, Pachter L, Poliakov A, Rubin EM, Dubchak I. VISTA: computational tools for comparative genomics. Nucleic Acids Res. 2004; 32: W273–W279. https://doi.org/10.1093/nar/gkh458 PMID: 15215394

26. Kel AE, Gössling E, Reuter I, Cheremushkin E, Kel-Margoulis OV, Wingender E. MATCH: A tool for searching transcription factor binding sites in DNA sequences. Nucleic Acids Res. 2003; 31: 3576–9. https://doi.org/10.1093/nar/gkg585 PMID: 12824369

27. Xi Y, Xu Q, Huang Q, Ma S, Wang Y, Han C, et al. Genome-wide association analysis reveals that EDNRB2 causes a dose-dependent loss of pigmentation in ducks. Bmc Genomics. 2021; 22: 381. https://doi.org/10.1186/s12864-021-07719-7 PMID: 34034661

28. Birlea SA, Jin Y, Bennett DC, Herbstman DM, Wallace MR, McCormack WT, et al. Comprehensive Association Analysis of Candidate Genes for Generalized Vitiligo Supports XBP1, FOXP3, and TSLP. J Invest Dermatol. 2011; 131: 371–381. https://doi.org/10.1038/jid.2010.337 PMID: 21085187

29. Hamburger V, Hamilton HL. A series of normal stages in the development of the chick embryo. J Morphol. 1951; 88: 49–92. https://doi.org/10.1002/jmor.1050880104 PMID: 24539719

30. Harris ML, Hall R, Erickson CA. Directing pathfinding along the dorsolateral path—the role of EDNRB2 and EphB2 in overcoming inhibition. Development. 2008; 135: 4113–4122. https://doi.org/10.1242/dev.023119 PMID: 19004859

31. Pla P, Alberti C, Solov'eva O, Pasdar M, Kunisada T, Larue L. Ednrb2 orients cell migration towards the dorsolateral neural crest pathway and promotes melanocyte differentiation. Pigm Cell Res. 2005; 18: 181–187. https://doi.org/10.1111/j.1600-0749.2005.00230.x PMID: 15892714

32. Kawasaki-Nishihara A, Nishihara D, Nakamura H, Yamamoto H. ET3/Ednrb2 signaling is critically involved in regulating melanophore migration in Xenopus. Dev Dynam. 2011; 240: 1454–1466. https://doi.org/10.1002/dvdy.22649 PMID: 21538684

33. Stringham SA, Mulroy EE, Xing J, Record D, Guernsey MW, Aldenhoven JT, et al. Divergence, Convergence, and the Ancestry of Feral Populations in the Domestic Rock Pigeon. Curr Biol. 2012; 22: 302–308. https://doi.org/10.1016/j.cub.2011.12.045 PMID: 22264611

34. Wu X, Yang Y, Xiang L, Zhang C. The fate of melanocyte: Mechanisms of cell death in vitiligo. Pigm Cell Melanoma R. 2021; 34: 256–267. https://doi.org/10.1111/pcmr.12955 PMID: 33346939

35. Varga L, Lénárt X, Zenke P, Orbán L, Hudák P, Ninausz N, et al. Being Merle: The Molecular Genetic Background of the Canine Merle Mutation. Genes-basel. 2020; 11: 660. https://doi.org/10.3390/genes11060660 PMID: 32560567

36. Tosney KW. Long-distance cue from emerging dermis stimulates neural crest melanoblast migration. Dev Dynam. 2004; 229: 99–108. https://doi.org/10.1002/dvdy.10492 PMID: 14699581

37. Lahav R, Dupin E, Lecoin L, Glavieux C, Champeval D, Ziller C, et al. Endothelin 3 selectively promotes survival and proliferation of neural crest-derived glial and melanocytic precursors in vitro. Proc National Acad Sci. 1998; 95: 14214–14219. https://doi.org/10.1073/pnas.95.24.14214 PMID: 9826680

38. Pla P, Larue L. Involvement of endothelin receptors in normal and pathological development of neural crest cells. Int J Dev Biology. 2003; 47: 315–25. PMID: 12895026

39. Oliphant LW. Observations on the Pigmentation of the Pigeon Iris. Pigm Cell Res. 1987; 1: 202–208. https://doi.org/10.1111/j.1600-0749.1987.tb00414.x PMID: 3508278

40. Yoshida H, Kunisada T, Kusakabe M, Nishikawa S, Nishikawa SI. Distinct stages of melanocyte differentiation revealed by anlaysis of nonuniform pigmentation patterns. Development. 1996; 122: 1207–1214. https://doi.org/10.1242/dev.122.4.1207 PMID: 8620847

41. Schöfer C, Frei K, Weipoltshammer K, Wachtler F. The apical ectodermal ridge, fibroblast growth factors (FGF-2 and FGF-4) and insulin-like growth factor I (IGF-I) control the migration of epidermal melanoblasts in chicken wing buds. Anat Embryol. 2001; 203: 137–146. https://doi.org/10.1007/s004290000148 PMID: 11218060

42. Miwa M, Inoue-Murayama M, Aoki H, Kunisada T, Hiragaki T, Mizutani M, et al. Endothelin receptor B2 (EDNRB2) is associated with the panda plumage colour mutation in Japanese quail: Quail plumage colour mutation associated with EDNRB2. Anim Genet. 2007; 38: 103–108. https://doi.org/10.1111/j.1365-2052.2007.01568.x PMID: 17313575

43. Li L, Li D, Liu L, Li S, Feng Y, Peng X, et al. Endothelin Receptor B2 (EDNRB2) Gene Is Associated with Spot Plumage Pattern in Domestic Ducks (Anas platyrhynchos). Plos One. 2015; 10: e0125883. https://doi.org/10.1371/journal.pone.0125883 PMID: 25955279

44. Kinoshita K, Akiyama T, Mizutani M, Shinomiya A, Ishikawa A, Younis HH, et al. Endothelin receptor B2 (EDNRB2) is responsible for the tyrosinase-independent recessive white (mo(w)) and mottled (mo) plumage phenotypes in the chicken. Plos One. 2014; 9: e86361. https://doi.org/10.1371/journal.pone.0086361 PMID: 24466053

45. Dao UM, Lederer I, Tabor RL, Shahid B, Graves CW, Seidel HS, et al. Stripes and loss of color in ball pythons (Python regius) are associated with variants affecting endothelin signaling. G3: GenesGenomesGenet. 2023; 13: jkad063. https://doi.org/10.1093/g3journal/jkad063 PMID: 37191439

46. Expression of Concern: Stripes and loss of color in ball pythons (Python regius) are associated with variants affecting endothelin signaling. G3: Genes, Genomes, Genet. 2023. https://doi.org/10.1093/g3journal/jkad182 PMID: 37611078

47. Spiewak JE, Bain EJ, Liu J, Kou K, Sturiale SL, Patterson LB, et al. Evolution of Endothelin signaling and diversification of adult pigment pattern in Danio fishes. Plos Genet. 2018; 14: e1007538. https://doi.org/10.1371/journal.pgen.1007538 PMID: 30226839

48. Parichy DM, Mellgren EM, Rawls JF, Lopes SS, Kelsh RN, Johnson SL. Mutational Analysis of Endothelin Receptor b1 (rose) during Neural Crest and Pigment Pattern Development in the Zebrafish Danio rerio. Dev Biol. 2000; 227: 294–306. https://doi.org/10.1006/dbio.2000.9899 PMID: 11071756

49. Braasch I, Volff J-N, Schartl M. The Endothelin System: Evolution of Vertebrate-Specific Ligand-Receptor Interactions by Three Rounds of Genome Duplication. Mol Biol Evol. 2009; 26: 783–799. https://doi.org/10.1093/molbev/msp015 PMID: 19174480

50. Jabeen R, Babar ME, Ahmad J, Awan AR. Novel mutations of endothelin-B receptor gene in Pakistani patients with Waardenburg syndrome. Mol Biol Rep. 2012; 39: 785–788. https://doi.org/10.1007/s11033-011-0799-x PMID: 21547364

51. Utzeri VJ, Ribani A, Fontanesi L. A premature stop codon in the TYRP1 gene is associated with brown coat colour in the European rabbit (Oryctolagus cuniculus). Anim Genet. 2014; 45: 600–603. https://doi.org/10.1111/age.12171 PMID: 24814776

52. Domyan ET, Guernsey MW, Kronenberg Z, Krishnan S, Boissy RE, Vickrey AI, et al. Epistatic and combinatorial effects of pigmentary gene mutations in the domestic pigeon. Curr Biology Cb. 2014; 24: 459–64. https://doi.org/10.1016/j.cub.2014.01.020 PMID: 24508169

53. Puckett EE, Davis IS, Harper DC, Wakamatsu K, Battu G, Belant JL, et al. Genetic architecture and evolution of color variation in American black bears. Curr Biol. 2023; 33: 86–97.e10. https://doi.org/10.1016/j.cub.2022.11.042 PMID: 36528024

54. Schmutz SM, Berryere TG, Goldfinch AD. TYRP1 and MC1R genotypes and their effects on coat color in dogs. Mamm Genome. 2002; 13: 380–387. https://doi.org/10.1007/s00335-001-2147-2 PMID: 12140685

55. Kijas JMH, Wales R, Törnsten A, Chardon P, Moller M, Andersson L. Melanocortin Receptor 1 (MC1R) Mutations and Coat Color in Pigs. Genetics. 1998; 150: 1177–1185. https://doi.org/10.1093/genetics/150.3.1177 PMID: 9799269

56. Fontanesi L, Tazzoli M, Beretti F, Russo V. Mutations in the melanocortin 1 receptor (MC1R) gene are associated with coat colours in the domestic rabbit (Oryctolagus cuniculus). Anim Genet. 2006; 37: 489–493. https://doi.org/10.1111/j.1365-2052.2006.01494.x PMID: 16978179

57. Nadeau NJ, Minvielle F, Mundy NI. Association of a Glu92Lys substitution in MC1R with extended brown in Japanese quail (Coturnix japonica). Anim Genet. 2006; 37: 287–289. https://doi.org/10.1111/j.1365-2052.2006.01442.x PMID: 16734695

58. Nachman MW, Hoekstra HE, D'Agostino SL. The genetic basis of adaptive melanism in pocket mice. Proc National Acad Sci. 2003; 100: 5268–5273. https://doi.org/10.1073/pnas.0431157100 PMID: 12704245

59. Guernsey MW, Ritscher L, Miller MA, Smith DA, Schöneberg T, Shapiro MD. A Val85Met Mutation in Melanocortin-1 Receptor Is Associated with Reductions in Eumelanic Pigmentation and Cell Surface Expression in Domestic Rock Pigeons (Columba livia). PLoS ONE. 2013; 8: e74475. https://doi.org/10.1371/journal.pone.0074475 PMID: 23977400

60. Cable J, Jackson IJ, Steel KP. Light (Blt), a Mutation That Causes Melanocyte Death, Affects Stria Vascularis Function in the Mouse Inner Ear. Pigm Cell Res. 1993; 6: 215–225. https://doi.org/10.1111/j.1600-0749.1993.tb00605.x PMID: 8248019

61. Thomas AC, Heux P, Santos C, Arulvasan W, Solanky N, Carey ME, et al. Widespread dynamic and pleiotropic expression of the melanocortin-1-receptor (MC1R) system is conserved across chick, mouse and human embryonic development. Birth Defects Res. 2018; 110: 443–455. https://doi.org/10.1002/bdr2.1183 PMID: 29316344

62. Braasch I, Brunet F, Volff J-N, Schartl M. Pigmentation Pathway Evolution after Whole-Genome Duplication in Fish. Genome Biol Evol. 2009; 1: 479–493. https://doi.org/10.1093/gbe/evp050 PMID: 20333216

63. Wittkopp PJ, Beldade P. Development and evolution of insect pigmentation: Genetic mechanisms and the potential consequences of pleiotropy. Semin Cell Dev Biol. 2009; 20: 65–71. https://doi.org/10.1016/j.semcdb.2008.10.002 PMID: 18977308

64. Hoekstra HE. Genetics, development and evolution of adaptive pigmentation in vertebrates. Heredity. 2006; 97: 222–234. https://doi.org/10.1038/sj.hdy.6800861 PMID: 16823403

65. Haddock J, Domyan ET. A DNA Replication Mechanism Can Explain Structural Variation at the Pigeon Recessive Red Locus. Biomol. 2022; 12: 1509. https://doi.org/10.3390/biom12101509 PMID: 36291717

66. Xie KT, Wang G, Thompson AC, Wucherpfennig JI, Reimchen TE, MacColl ADC, et al. DNA fragility in the parallel evolution of pelvic reduction in stickleback fish. Science. 2019; 363: 81–84. https://doi.org/10.1126/science.aan1425 PMID: 30606845

67. Boer EF, Hollebeke HFV, Maclary ET, Holt C, Yandell M, Shapiro MD. A ROR2 coding variant is associated with craniofacial variation in domestic pigeons. Curr Biol. 2021; 31: 5069–5076.e5. https://doi.org/10.1016/j.cub.2021.08.068 PMID: 34551284

68. Domyan ET, Kronenberg Z, Infante CR, Vickrey AI, Stringham SA, Bruders R, et al. Molecular shifts in limb identity underlie development of feathered feet in two domestic avian species. Elife. 2016; 5: e12115. https://doi.org/10.7554/eLife.12115 PMID: 26977633

69. Auwera GA, Carneiro MO, Hartl C, Poplin R, Angel G del, Levy-Moonshine A, et al. From FastQ Data to High-Confidence Variant Calls: The Genome Analysis Toolkit Best Practices Pipeline. Curr Protoc Bioinform. 2013; 43: 11.10.1–11.10.33. https://doi.org/10.1002/0471250953.bi1110s43 PMID: 25431634

70. Holt C, Campbell M, Keays DA, Edelman N, Kapusta A, Maclary E, et al. Improved Genome Assembly and Annotation for the Rock Pigeon (Columba livia). G3 Amp 58 Genes Genomes Genetics. 2018; 8: 1391–1398. https://doi.org/10.1534/g3.117.300443 PMID: 29519939

71. Bruders R, Hollebeke HV, Osborne EJ, Kronenberg Z, Maclary E, Yandell M, et al. A copy number variant is associated with a spectrum of pigmentation patterns in the rock pigeon (Columba livia). Plos Genet. 2020; 16: e1008274. https://doi.org/10.1371/journal.pgen.1008274 PMID: 32433666

72. Vickrey AI, Bruders R, Kronenberg Z, Mackey E, Bohlender RJ, Maclary ET, et al. Introgression of regulatory alleles and a missense coding mutation drive plumage pattern diversity in the rock pigeon. Elife. 2018; 7: e34803. https://doi.org/10.7554/eLife.34803 PMID: 30014848

73. Shapiro MD, Kronenberg Z, Li C, Domyan ET, Pan H, Campbell M, et al. Genomic diversity and evolution of the head crest in the rock pigeon. Sci New York N Y. 2013; 339: 1063–7. https://doi.org/10.1126/science.1230422 PMID: 23371554

74. Garrison E, Kronenberg ZN, Dawson ET, Pedersen BS, Prins P. Vcflib and tools for processing the VCF variant call format. Biorxiv. 2021; 2021.05.21.445151. https://doi.org/10.1101/2021.05.21.445151

75. Schneider CA, Rasband WS, Eliceiri KW. NIH Image to ImageJ: 25 years of image analysis. Nat Methods. 2012; 9: 671–675. https://doi.org/10.1038/nmeth.2089 PMID: 22930834

76. R Core Team. R: A Language and Environment for Statistical Computing. R Foundation for Statistical Computing. 2020. https://www.R-project.org/

77. Elshire RJ, Glaubitz JC, Sun Q, Poland JA, Kawamoto K, Buckler ES, et al. A Robust, Simple Genotyping-by-Sequencing (GBS) Approach for High Diversity Species. Plos One. 2011; 6: e19379. https://doi.org/10.1371/journal.pone.0019379 PMID: 21573248

78. Martin M. Cutadapt removes adapter sequences from high-throughput sequencing reads. Embnet J. 2011; 17: 10–12. https://doi.org/10.14806/ej.17.1.200

79. Langmead B, Salzberg SL. Fast gapped-read alignment with Bowtie 2. Nat Methods. 2012; 9: 357–359. https://doi.org/10.1038/nmeth.1923 PMID: 22388286

80. Catchen J, Hohenlohe PA, Bassham S, Amores A, Cresko WA. Stacks: an analysis tool set for population genomics. Mol Ecol. 2013; 22: 3124–3140. https://doi.org/10.1111/mec.12354 PMID: 23701397

81. Broman KW, Wu H, Sen Ś, Churchill GA. R/qtl: QTL mapping in experimental crosses. Bioinformatics. 2003; 19: 889–890. https://doi.org/10.1093/bioinformatics/btg112 PMID: 12724300

82. Lincoln SE, Lander ES. Systematic detection of errors in genetic linkage data. Genomics. 1992; 14: 604–610. https://doi.org/10.1016/s0888-7543(05)80158-2 PMID: 1427888

83. Quinlan AR, Hall IM. BEDTools: a flexible suite of utilities for comparing genomic features. Bioinformatics. 2010; 26: 841–842. https://doi.org/10.1093/bioinformatics/btq033 PMID: 20110278

84. Dobin A, Davis CA, Schlesinger F, Drenkow J, Zaleski C, Jha S, et al. STAR: ultrafast universal RNA-seq aligner. Bioinformatics. 2013; 29: 15–21. https://doi.org/10.1093/bioinformatics/bts635 PMID: 23104886

85. Liao Y, Smyth GK, Shi W. featureCounts: an efficient general purpose program for assigning sequence reads to genomic features. Bioinformatics. 2014; 30: 923–930. https://doi.org/10.1093/bioinformatics/btt656 PMID: 24227677

86. Love MI, Huber W, Anders S. Moderated estimation of fold change and dispersion for RNA-seq data with DESeq2. Genome Biol. 2014; 15: 550. https://doi.org/10.1186/s13059-014-0550-8 PMID: 25516281

87. Madeira F, Park Y mi, Lee J, Buso N, Gur T, Madhusoodanan N, et al. The EMBL-EBI search and sequence analysis tools APIs in 2019. Nucleic Acids Res. 2019; 47: W636–W641. https://doi.org/10.1093/nar/gkz268 PMID: 30976793

88. Waterhouse AM, Procter JB, Martin DMA, Clamp M, Barton GJ. Jalview Version 2—a multiple sequence alignment editor and analysis workbench. Bioinformatics. 2009; 25: 1189–1191. https://doi.org/10.1093/bioinformatics/btp033 PMID: 19151095

89. Robinson JT, Thorvaldsdóttir H, Winckler W, Guttman M, Lander ES, Getz G, et al. Integrative genomics viewer. Nat Biotechnol. 2011; 29: 24–26. https://doi.org/10.1038/nbt.1754 PMID: 21221095

90. Li H, Handsaker B, Wysoker A, Fennell T, Ruan J, Homer N, et al. The Sequence Alignment/Map format and SAMtools. Bioinformatics. 2009; 25: 2078–2079. https://doi.org/10.1093/bioinformatics/btp352 PMID: 19505943

91. Altschul SF, Gish W, Miller W, Myers EW, Lipman DJ. Basic local alignment search tool. J Mol Biol. 1990; 215: 403–410. https://doi.org/10.1016/S0022-2836(05)80360-2 PMID: 2231712

92. Grabherr MG, Haas BJ, Yassour M, Levin JZ, Thompson DA, Amit I, et al. Full-length transcriptome assembly from RNA-Seq data without a reference genome. Nat Biotechnol. 2011; 29: 644–652. https://doi.org/10.1038/nbt.1883 PMID: 21572440

93. Madeira F, Pearce M, Tivey ARN, Basutkar P, Lee J, Edbali O, et al. Search and sequence analysis tools services from EMBL-EBI in 2022. Nucleic Acids Res. 2022; 50: W276–W279. https://doi.org/10.1093/nar/gkac240 PMID: 35412617